DuoHexaBody-CD37 induces direct cytotoxic signaling in diffuse large B-cell lymphoma

Simar Pal Singh[1], Kumar Mangalam[1,#], Michelle D. van den Beukel[1,#], Sjoerd van Deventer[1], Marije B. Overdijk[2], M. Guy Roukens[2], Kim C.M. Santegoets[2], Esther C.W. Breij[2], Martin ter Beest[1], Willem P. J. Cox[1], Annemiek B. van Spriel[1,*]

[1] Department of Medical BioSciences, Radboud Institute for Medical Innovation, Radboud University Medical Center, Nijmegen, the Netherlands. [2] Genmab, Utrecht, the Netherlands.

# These authors contributed equally.

* Corresponding author: Annemiek van Spriel (annemiek.vanspriel@radboudumc.nl)

Phone number: +31 24317600

Running title: Cytotoxic signaling by DuoHexaBody-CD37

Abstract

Diffuse large B-cell lymphoma (DLBCL) is a common aggressive form of Non-Hodgkin lymphoma. Tetraspanin CD37 is highly expressed on mature B cells and being studied as a therapeutic target for NHL, including DLBCL. DuoHexaBody-CD37 is a biparatopic antibody with an E430G hexamerization-enhancing mutation targeting two non-overlapping CD37 epitopes shown to promote complement-dependent cytotoxicity. However, the impact of DuoHexaBody-CD37 on direct cytotoxic signaling has not yet been studied. Here we demonstrate that DuoHexaBody-CD37 induces direct cytotoxicity in DLBCL-derived tumor cell lines independent of the subtype. DuoHexaBody-CD37 induced significant CD37 clustering and was retained at the cell surface in contrast to rituximab, which was internalized. Unbiased screening identified the modulation of 26 (phospho)proteins upon DuoHexaBodyCD37 treatment of primary B cells or DLBCL cells. Whereas DLBCL cells predominantly upregulated p-SHP1(Y564) upon DuoHexaBody-CD37 treatment, primary B cells showed significantly increased p-AKT(S473) and MAPK signaling which is linked to cell survival. Studies using CD37-mutants identified the N-terminus to be involved in DuoHexaBody-CD37-induced signaling. Finally, DuoHexaBody-CD37 treatment inhibited cytokine pro-survival signaling in DLBCL cells. These findings provide novel insights into the signaling functions of CD37 upon DuoHexaBody-CD37 treatment, and open up opportunities for developing CD37-targeted immunotherapy in combination with small molecule inhibitors to maximize tumor cell death.

Introduction

Diffuse large B-cell lymphoma (DLBCL), an aggressive type of mature B-cell lymphoma, accounts for approximately one third of Non-Hodgkin lymphoma (NHL) cases. DLBCL arises from mature B cells in the lymph node, and comprises a heterogenous group of tumors that can be classified according to cell-of-origin (germinal-center B-cell (GCB) derived and activated B-cell (ABC) subtypes). In addition, recent comprehensive molecular profiling has identified five to seven genetic subtypes that share similar oncogenic pathways (reviewed in [1]). A large fraction of DLBCL patients (up to 40%) do not respond or relapse after first line treatment with chemotherapy (cyclophosphamide, hydroxydaunorubicin, vincristine sulphate (Oncovin), and prednisone: CHOP) and immunotherapy (rituximab). Rituximab and also next-generation antibodies (ofatumumab) target CD20 at the plasma membrane of DLBCL [2], however decreased expression of CD20 is related to inferior clinical outcome after treatment with R-CHOP [3,4,5]. Thus, targeting alternative B-cell membrane proteins and development of novel immunotherapies are needed to improve clinical outcomes of patients with relapsed/refractory DLBCL [6,7].

CD37 is a tetraspanin protein with four-transmembrane domains, which is predominantly expressed by mature B cells [8–10]. Tetraspanins interact with immune receptors on the same cell (in cis) and control membrane organization in lymphocytes [11–13]. CD37 is absent on progenitor B cells and terminally differentiated plasma cells making it an ideal target for mature B cell malignancies [14,15,16]. In DLBCL patients, CD37 was reported to be an independent prognostic factor for both GCB and ABC subtypes [4]. In line with these findings, CD37-deficient mice show defects in humoral and cellular immune responses, and spontaneously develop mature B-cell lymphoma, which is dependent on IL-6 [17]. IL-6 signals through the IL-6 receptor complex that activates AKT kinase and STAT3 signaling stimulating

61 cell survival and proliferation. IL-6 signaling has been reported to be a critical driver in the
62 tumor microenvironment and a negative prognostic factor in diffuse large B-cell lymphoma
63 [18].
64 CD37 is under preclinical and clinical investigation as novel therapeutic target for BNHL,
65 including antibody-based and chimeric antigen receptor (CAR) T-cell therapies [19–23,24].
66 DuoHexaBody-CD37 (GEN3009) is a novel biparatopic immunoglobulin G1 (IgG1) with a point
67 mutation in the Fc-domain (E430G) that enhances antibody hexamerization upon binding to
68 the cell surface [25]. This facilitates C1q binding and results in potent complement-dependent
69 cytotoxicity (CDC). In addition DuoHexaBody-CD37 can induce Fc-gamma receptor (FcγR)
70 mediated antibody-dependent cellular cytotoxicity (ADCC) and phagocytosis (ADCP) by
71 effector cells. DuoHexaBody-CD37 mediates superior CDC in patient-derived DLBCL cells ex
72 vivo compared to CD20 monoclonal antibodies as shown in preclinical studies [26].
73 In B cells, CD37 has been reported to connect to intracellular signaling pathways via
74 its two intracellular tails [9,27]. The N-terminal tail of CD37 contains a potential 'ITIM-like' motif
75 that may induce SHP1 signaling, whereas the C-terminal tail of CD37 bears a predicted 'ITAM-
76 like' motif that may stimulate AKT kinase-dependent survival [27]. Here we investigated
77 whether DuoHexaBody-CD37 is capable of inducing intracellular signaling that induces cell
78 death of malignant B cells. We report that DuoHexaBody-CD37 mediates direct CD37-
79 mediated signaling and evokes tumor cytotoxicity in DLBCL-derived tumor cells, independent
80 of the presence of complement. DuoHexaBody-CD37 modulated the PI3K-AKT and MAPK
81 signaling pathways, with differences observed between primary B cells and DLBCL tumor
82 cells. Moreover, DuoHexaBody-CD37 inhibited IL-4-dependent p-STAT6 and IL-21-dependent
83 p-STAT3 signaling in DLBCL cells. In conclusion, this study shows a novel mechanism of action

84 of DuoHexaBody-CD37, and provides more insight into CD37 as therapeutic target for B cell

85 malignancies.

86 # Results

87 **DuoHexaBody-CD37 mediates direct cytotoxicity in DLBCL cell lines**

88 Induction of apoptosis in B cell leukemia and lymphomas has been reported for therapeutic
89 antibodies such as obinutuzumab [28], alemtuzumab [29], otlertuzumab [30], and rituximab [31]. To
90 investigate the direct cytotoxic potential of DuoHexaBody-CD37, DLBCL-derived cell lines
91 classified as GCB (Oci-Ly8 and Oci-Ly7), ABC (HBL-1 and U2932) and Burkitt lymphoma-
92 derived cell lines (BJAB, Daudi) were treated with DuoHexaBody-CD37 in the absence of
93 complement, and with or without an Fc-targeting F(ab)2-fragment (a-Fc) to facilitate Fc-
94 mediated crosslinking. Whereas the viability of Burkitt lymphoma-derived cell lines (BJAB and
95 Daudi) was not significantly affected by DuoHexaBody-CD37 and Fc-crosslinking treatment,
96 all tested DLBCL-derived cell lines showed >25% reduction in viability after DuoHexaBody-
97 CD37 treatment with a-Fc (Figure 1A). We confirmed that apoptosis was the mechanism of
98 cell death by Annexin V and 7-AAD staining in Oci-Ly7 and HBL1 cell lines upon Fc-crosslinking
99 of DuoHexaBody-CD37 (Supplementary Figure 1A). Notably, differences in viability loss after
100 treatment did not correlate with differences in CD37 membrane expression in the tested cell
101 lines (Supplementary Figure 1B). To investigate the physiological relevance of Fc-crosslinking
102 mediated DuoHexaBody-CD37 induced killing, cytotoxicity assays of DLBCL cell lines were
103 performed using peripheral blood mononuclear cells (PBMCs) expressing Fcɣ receptors
104 (FcɣR). In these assays, PBMCs were pre-fixed to prevent FcɣR signaling and to avoid any
105 influence of ADCC/ADCP as previously shown with DuoHexaBody-CD37 [25]. DuoHexaBody-
106 CD37 treatment resulted in significantly increased direct cytotoxicity of DLBCL cells compared
107 to untreated cells in presence of PBMCs as source for Fc-crosslinking for all donors tested
108 (Figure 1B). Collectively, these results show induction of direct cytotoxicity by DuoHexaBody-
109 CD37 treatment with Fc crosslinking in different DLBCL cells. To further investigate the

110 contribution of specific FcγRs in effector cell mediated Fc-crosslinking, total PBMCs were
111 compared with defined immune cell subsets: B cells (expressing FcγRIIb), NK cells (expressing
112 FcγRIIIa and FcγRIIc), monocytes (expressing FcγRI, FcγRIIa, FcγRIIb, and FcγRIIIa), and T cells
113 with no confirmed expression of FcγR. All immune cell subsets expressing FcγRs led to similar
114 or greater direct cytotoxicity of DLBCL cells compared with the total PBMC pool (Figure 1C).
115 These results indicate that DuoHexaBody-CD37-induced killing through Fc-mediated
116 crosslinking is not dependent on the expression of specific FcγR subtypes.
117

118 **DuoHexaBody-CD37 induces CD37 clustering without modulating CD37 cell surface**
119 **expression**

120 CD37 is involved in the spatial organization of the B-cell plasma membrane by forming
121 tetraspanin nanodomains [13], therefore we investigated CD37 membrane clustering on
122 DuoHexaBody-CD37-treated tumor cells compared to tumor cells treated with the IgG1
123 isotype control antibody with and without a-Fc mediated crosslinking, respectively. Whereas
124 CD37 surface expression was the same in both samples, the clustering of CD37 on tumor cells
125 (measured by fluorescence intensity/area) was significantly higher upon DuoHexaBody-CD37
126 treatment than isotype control antibody treatment (Figure 2A, B). Interestingly,
127 DuoHexaBody-CD37-mediated clustering of CD37 was observed in both Burkitt cells (BJAB)
128 (Figure 2A) and DLBCL (Oci-Ly8) (Figure 2B) even in absence of Fc-crosslinker . Upon
129 crosslinking, clustering of CD37 increased in both cell lines, however the effect was more
130 pronounced in BJAB cells compared to Oci-Ly8. Thus, DuoHexaBody-CD37 induces potent
131 CD37 membrane clustering at the cell surface of malignant B cells with and without Fc-
132 mediated crosslinking.

133 Since the efficacy of rituximab can be negatively impacted by induction of CD20
134 internalization, leading to loss of CD20 expression at the cell surface [32,33], we investigated
135 whether DuoHexaBody-CD37 affected CD37 cell surface accessibility. We observed no
136 changes in surface CD37 expression upon DuoHexaBody-CD37 treatment in all cell lines
137 tested, in contrast to CD20 expression upon rituximab treatment, which was decreased on
138 DAUDI, Oci-Ly8 and Oci-Ly7 cells (Figure 2C). We next assessed CD37 surface availability with
139 and without Fc-crosslinking of DuoHexaBody-CD37 and observed no consistent reduction in
140 CD37 surface availability upon crosslinking (Supplementary Figure 2). Thus, the efficacy of
141 DuoHexaBody-CD37 is not affected by loss of CD37 through internalization of surface
142 molecules.
143
144 **DuoHexaBody-CD37 treatment results in activation of multiple downstream signaling**
145 **pathways**
146 Next, we focused on investigating mechanisms underlying the direct cytotoxicity upon
147 DuoHexaBody-CD37 treatment by analyzing DuoHexaBody-CD37-induced downstream
148 signaling using high throughput Reverse Phase Protein Array (RPPA) [34]. This technique
149 enables simultaneous unbiased measurement of 484 proteins (102 phospho targets and 382
150 total proteins) in multiple samples at once. For this analysis primary B cells (purified CD19+ B
151 cells from PBMCs) and two DLBCL-derived cell lines (Oci-Ly7 and U2932) were treated with
152 DuoHexaBody-CD37 in the presence or absence of Fc-crosslinker and compared to untreated
153 samples from each cell type. Principal component analysis on all tested proteins in RPPA
154 identified 3 separate clusters correlating with the different cell models (Supplementary Figure
155 3). Compared to respective untreated controls, 26 phosphoproteins showed at least a two-
156 fold change in either of the three cell models tested upon DuoHexaBody-CD37 treatment

157 (Figure 3A). Pathway analysis on all 26 phospho-sites identified PI3K/AKT/MTOR signaling as
158 the most significantly enriched pathway upon DuoHexaBody-CD37 treatment (Figure 3B). In
159 addition, some of these signaling proteins are downstream of B cell receptor (BCR) signaling
160 and RAS signaling pathways, which have been reported to be essential for B cell survival and
161 lymphomagenesis [35,36].

162 Next, the effect of DuoHexaBody-CD37 treatment on primary B cells versus tumor cells was
163 studied by focusing on those phosphoproteins that showed approximately two-fold
164 upregulation in signal compared to untreated controls. Primary B cells showed upregulation
165 of multiple phosphoproteins upon DuoHexaBody-CD37 treatment including p-AKT, p-FAK,
166 pSrc and p-Shc. In DLBCL cells, different phosphoproteins (p-RPA32, p-DAPK1, p-PAK, p-PI3K
167 and p-FRS-alpha) were upregulated upon DuoHexaBody-CD37 treatment. The list of targets
168 and fold changes can be found in Supplementary Table 1.

169 To validate these results, we analyzed different targets within the three main signaling
170 pathways that came out of the RPPA analysis: the PI3K/AKT pathway, BCR pathway and
171 MAPK/ERK pathway using phosphoflow analysis. Anti-BCR (IgM) was used as stimulation
172 control in the phosphoflow studies. We confirmed specific upregulation of p-AKT(S473) in
173 primary B cells upon treatment with DuoHexaBody-CD37 in the presence of Fc-crosslinker
174 compared to untreated cells (Figure 3C). In DLBCL cell lines, upregulation of p-AKT(S473) was
175 not specific for DuoHexaBody-CD37 treatment as this was already observed in presence of
176 the Fc-crosslinker only (Figure 3C). These data indicate a differential role of DuoHexaBody-
177 CD37 mediated signaling in primary B cells versus DLBCL which could be partially explained
178 by constitutive activation of the PI3K-AKT pathway in DLBCL [37]. As engagement of cell death
179 pathways in CLL cells was shown to be dependent on SHP1 recruitment and activation via
180 CD37 N-terminus [27], we additionally assessed p-SHP1(Y564) status upon DuoHexaBody-CD37

181 treatment of primary B cells and DLBCL cells via phosphoflow. Compared to untreated cells,
182 DuoHexaBody-CD37 treatment in the presence of Fc-crosslinker induced significant
183 upregulation of p-SHP1(Y564) in both primary B cells and DLBCL cells (Figure 3C,
184 Supplementary Figure 4A).
185 To analyze phosphoproteins downstream of the BCR, we studied p-SYK, p-BTK, pPLCγ2 and p-
186 PKC in primary B cells and DLBCL cells by phosphoflow. p-SYK was observed to be upregulated
187 only after BCR stimulation (anti-IgM), but not after DuoHexaBody-CD37 treatment of primary
188 B cells or DLBCL cells (Figure 3C). On other hand, p-PLCγ2(Y759) and p-BTK(Y223) were
189 specifically upregulated in DLBCL cells upon treatment with DuoHexaBody-CD37 in the
190 presence of Fc-crosslinker (Figure 4A, Supplementary Figure 4B). Next, we analyzed the
191 MAPK signaling pathway and observed p-P38 to be specifically upregulated in primary B cells,
192 but not in DLBCL cells, upon DuoHexaBody-CD37 treatment in the presence of Fc-crosslinker
193 (Figure 4B, Supplementary Figure 4C). Similarly, ERK phosphorylation was upregulated in
194 primary B cells upon DuoHexaBody-CD37 treatment in the presence of Fc crosslinker, in
195 contrast to DLBCL cells (Figure 4B, Supplementary Figure 4C). Taken together, DuoHexaBody-
196 CD37 treatment activates different signaling cascades in primary B cells versus DLBCL-derived
197 tumor cells.
198
199 **CD37 N-terminus is involved in DuoHexaBody-CD37-mediated signaling**
200 As tyrosine phosphorylation of the CD37 N-terminus was reported to be crucial in CD37
201 mediated signaling [27], we examined the involvement of CD37 N-terminus in
202 DuoHexaBodyCD37-induced signaling. In these experiments, B-ALL cells (NALM6) with low
203 endogenous CD37 expression were used to investigate various CD37 mutant constructs [27].
204 NALM6 cells transfected with wild type CD37 (CD37-WT), or with CD37 carrying either the

205 Tyr13 to phenylalanine mutation (CD37-Y13F) or a deletion of Tyr13 residue (CD37-ΔY13) in
206 the cytosolic region of the CD37 molecule were generated. Cell surface expression of CD37-
207 WT and both mutant variants was validated by flow cytometry (Figure 5A). DuoHexaBody-
208 CD37 treatment in the presence of Fc-crosslinker resulted in significant upregulation of p-
209 AKT(S473) and p-SHP1(Y564) in NALM6 cells expressing CD37-WT compared to treatment
210 with only the crosslinker (Figure 5B, C) in line with findings observed in the DLBCL-derived
211 cell lines (Figure 3C). Interestingly, deleting Tyr13 (CD37-ΔY13) completely impaired p-
212 AKT(S473) and p-SHP1(Y564) upregulation, whereas mutating Tyr13 (CD37-Y13F) did not
213 result in major changes upon DuoHexaBody-CD37 treatment in the presence of Fc-crosslinker
214 (Figure 5B, C). In conclusion, these data validate active CD37 downstream signaling upon
215 target engagement with DuoHexaBody-CD37 in the presence of Fc-crosslinker, and suggest
216 the involvement of the CD37 N-terminus in mediating direct cytotoxic signaling. Since p-SHP1
217 upregulation was observed specifically in DuoHexaBody-CD37-treated cells upon Fc
218 crosslinking, and SHP1 signaling was abolished when CD37-Y13 was mutated, we next
219 investigated whether SHP1 knockout in Oci-Ly7 and HBL1 cells (Supplementary Figure 5A)
220 affected the induction of direct cytotoxicity. No change in cytotoxicity was observed in either
221 of the two cell lines following knockout of SHP1 (Supplementary Figure 5B), indicating that
222 SHP1 signaling induced by DuoHexaBody-CD37 Fc-crosslinking does not directly contribute to
223 the enhanced cytotoxicity.
224

225 **DuoHexaBody-CD37 treatment abrogates cytokine mediated pro-survival signaling in**
226 **DLBCL cells**

227 As cells within the DLBCL tumor microenvironment can stimulate tumor growth by supplying
228 cytokines [38] and CD37 has been reported to inhibit IL-6 signaling [17], we next investigated the

229 impact of DuoHexaBody-CD37 treatment on cytokine-mediated oncogenic signaling.
230 Different DLBCL cell lines were treated with DuoHexaBody-CD37 in absence or presence of
231 Fc-crosslinker, followed by stimulation with either recombinant human IL-4 (rh-IL4), IL-6
232 (rhIL6) or IL-21 (rh-IL21) and analyzed for p-STAT activation by phosphoflow. These cytokines
233 were selected because of their pro-tumorigenic role in DLBCL and other hematological
234 cancers [18, 38,39,40,41]. All tested DLBCL-derived tumor cell lines showed a significant increase in
235 the level of p-STAT6 upon rh-IL-4 stimulation. Pre-treatment with DuoHexaBody-CD37 in the
236 presence of a crosslinker showed a significant decrease in percentage p-STAT6-positive tumor
237 cells upon stimulation with rh-IL-4 (Figure 6A) in contrast to controls (untreated or cells
238 treated with DuoHexaBody-CD37 or Fc-crosslinker alone). Next, IL-6-induced p-STAT3
239 signaling was investigated in HBL-1 cells, as the other DLBCL-derived tumor cell lines did not
240 respond to IL-6 (data not shown). A two-fold increase in percentage p-STAT3-positive HBL-1
241 cells was observed upon rh-IL6 stimulation. Interestingly, treatment with DuoHexaBody-CD37
242 in the presence of a crosslinker also decreased the percentage of p-STAT3-positive HBL-1 cells
243 compared to controls (untreated or cells treated with DuoHexaBody-CD37 or crosslinker
244 alone) although this was not significant (Figure 6B). Finally, IL-21-induced p-STAT3 signaling
245 was investigated in all four cell lines. Both ABC-DLBCL derived tumor cells (HBL-1 and U2932)
246 showed a > four-fold increase in the percentage of p-STAT3-positive cells, while the effect was
247 more modest in the GCB-DLBCL-derived tumor cells (Oci-Ly8) showing a two-fold increase in
248 p-STAT3 signal. Oci-Ly7 cells did not respond to IL-21 (data not shown). DuoHexaBody-CD37
249 treatment in the presence of Fc-crosslinker showed in all three IL-21 responsive cell lines a
250 significant decrease in the percentage of p-STAT3-positive cells upon rh-IL21 stimulation
251 (Figure 6C) in line with IL-4 and IL-6 stimulation. Collectively, these experiments show that

252 DuoHexaBody-CD37 treatment in the presence of Fc-crosslinker inhibits cytokine-mediated

253 pro-survival signaling in the DLBCL tumor microenvironment.

254

255 ## Discussion

256 A large fraction (~40%) of patients with DLBCL do not respond to or relapse after first-line
257 treatment with standard immunochemotherapy (R-CHOP), emphasizing the unmet medical
258 need to develop new therapies for DLBCL. Tetraspanins have gained strong interest as
259 therapeutic targets in different cancer types due to their capacity to regulate cell
260 proliferation, adhesion and migration. Importantly, many tumor cells have altered cell surface
261 expression of tetraspanins making them attractive targets for the treatment of cancer [16,42].
262 For example, CD151 is upregulated in carcinomas and CD151 stimulates both primary tumor
263 growth and the metastatic cascade through its interaction with β1 integrins [42,43]. In B cell
264 lymphoma, CD81 has been reported to be highly expressed by malignant cells from patients
265 with B-NHL, and CD81-specific antibodies have been reported to be cytotoxic for such cells
266 while sparing normal B cells [44]. CD37 represents an alternative therapeutic target for B-NHL
267 because of its specific membrane expression on mature B cells, and its prognostic value in
268 DLBCL and follicular lymphoma [4,45]. DuoHexaBody-CD37 has been previously reported to
269 mediate cytotoxicity of DLBCL cells via different mechanisms of action: complement (CDC)
270 and effector cell-mediated killing (ADCC/ADCP) [25,26]. Here, we report an additional
271 mechanism of action of DuoHexaBody-CD37: CD37-mediated direct cytotoxicity which is
272 independent of complement. Direct antibody-mediated killing may be particularly important
273 in the DLBCL tumor microenvironment when complement is not available or inhibited.
274 Complement has a dual role in tumors including hematological malignancies. The protective
275 role of complement in antibody-mediated CDC has been well-established. However, more
276 recent studies have provided evidence that tumors can hijack the complement components
277 by cell surface expression of C1q, C3a and C5a receptors that promotes tumor growth and

278 progression [46,47]. In addition, lymphoma cells can upregulate complement regulatory proteins
279 (CRPs: CD46, CD55 and CD59) to escape from antibody mediated CDC [48]. Although no direct
280 correlation was found between DuoHexaBody-CD37-induced CDC and expression of CRPs in
281 vitro [26], expression of CD59 has been shown to predict clinical outcome in DLBCL patients
282 treated with R-CHOP [49]. In addition, the presence of regulatory myeloid cells (tumor-
283 associated neutrophils, myeloid-derived suppressor cells) in the tumor microenvironment
284 has been associated with immune suppression and poor prognosis in lymphoma (reviewed in
285 [38,50]). These tumor-infiltrating myeloid cells stimulate tumor growth and may impair
286 ADCC/ADCP activity of therapeutic antibodies [51]. Lastly, DLBCL cells have been shown to
287 upregulate CD47 to protect themselves from ADCC and ADCP [52]. Taken together, inhibition of
288 complement activation by tumor cells or ineffective ADCC/ADCP may limit efficacy of
289 antibody-based immunotherapies for hematological malignancies.

290 Since decreased expression of CD20 is related to inferior clinical outcome of DLBCL
291 patients after treatment with R-CHOP, DuoHexaBody-CD37 treatment may be more potent
292 compared to CD20-targeting therapies in DLBCL. Supporting this, we observed no/minimal
293 internalization of CD37 by DuoHexaBody-CD37 in contrast to rituximab-induced CD20
294 internalization. We observed that DLBCL cells were more sensitive to DuoHexaBody-
295 CD37mediated cytotoxicity than Burkitt cells, a difference that cannot be explained by
296 variations in CD37 surface expression or clustering. It is possible that Burkitt cells rely on
297 other oncogenic signaling pathways (i.e. MYC-driven) compared to DLBCL cells.

298 The activation of multiple intracellular signaling pathways, including PI3K-AKT and
299 RAS-MAPK that play a central role in cancer, was observed upon DuoHexaBody-CD37
300 treatment of DLBCL cells. This was dependent on Fc-crosslinking of DuoHexaBody-CD37,
301 which is in line with former studies using CD37-specific small modular

302 immunopharmaceuticals (CD37-SMIP) [53,54]. In vivo crosslinking could be facilitated by
303 effector cells expressing Fc receptors, as evidenced by the observed direct cytotoxicity of
304 DuoHexaBody-CD37 in tumor cells in the presence of PBMCs. This did not require FcγR
305 mediated signaling or effector cell function (degranulation, trogocytosis) as fixed PBMCs
306 could be used to facilitate the crosslinking. CD37 can activate and inhibit AKT kinase through
307 its two intracellular tails that contain ITIM-like and ITAM-like motifs [27]. Different mechanisms
308 of direct tumor cell death by antibodies have been reported, including apoptosis, necrosis,
309 pyroptosis and necroptosis. We identified apoptosis as the mechanism underlying
310 DuoHexaBody-CD37–induced killing of DLBCL cells, and future studies, and future studies are
311 needed to determine whether any of the other mechanisms are involved as well.
312 mechanisms underlie DuoHexaBody-CD37-induced killing of DLBCL cells. Interestingly,
313 increased p-AKT was observed in primary B cells upon DuoHexaBody-CD37 treatment in
314 contrast to malignant B cells, indicating that primary B cells may be less sensitive to direct
315 killing than lymphoma cells. Our results show that DuoHexaBody-CD37 directly affects the
316 membrane-proximal signaling protein AKT which may provide new opportunities for
317 combination therapies in DLBCL [55]. For example, studies combining CD37-targeting
318 antibodies with PI3K inhibitors [56,57] or cell cycle kinase inhibitors [58] demonstrated enhanced
319 tumor cell death. We also observed p-BTK and p-PLCy upregulation in ABC-DLBCL upon
320 DuoHexaBody-CD37 treatment, which could provide a rational to combine
321 DuoHexaBodyCD37 with ibrutinib in ABC-DLBCL where BTK inhibition is already more
322 effective compared to GBC-DLBCL [59,60]. DuoHexaBody-CD37 treatment also led to an increase
323 in SHP1 mediated signaling, however we could not confirm a direct role of SHP1 signaling in
324 DuoHexaBody-CD37-mediated cytotoxicity. DLBCL cells may undergo signal rewiring upon
325 SHP1 knockdown by altered levels of p-AKT, p-STAT3, and p-STAT6, or SHP2 may compensate

326 for the loss of SHP1. It is currently unclear what the biological implications are of the
327 increased SHP1 signaling observed upon treatment with DuoHexaBody-CD37 in DLBCL cells.
328 Moreover, DuoHexaBody-CD37 was found to be particularly effective in
329 downregulating p-STAT3 and p-STAT6 in presence of IL-21 and IL-4, respectively. Within the
330 DLBCL tumor microenvironment, these cytokines actively contribute to cancer pathogenesis
331 in ABC-DLBCL [18,38,39,40,41]. p-STAT3 downregulation upon DuoHexaBody-CD37 treatment in
332 presence of IL-6 requires further investigation in additional IL-6-responsive cell lines, as HBL1
333 was the only IL-6-responsive lymphoma cell line tested in this study. IL-6 levels in serum are
334 associated with adverse clinical outcome in DLBCL, and we previously reported that CD37
335 inhibits IL-6 receptor signaling through SOCS3 [17]. In line with this, patients with CD37-
336 negative DLBCL present with higher IL-6 levels in serum and tumors which is associated with
337 inferior clinical outcome [17]. CD37 is an independent prognostic factor in DLBCL, irrespective
338 of DLBCL subset [4], which has been confirmed in patients with follicular lymphoma [45]. We
339 anticipate that targeting CD37, especially in the presence of classical chemotherapy and/or
340 targeted drugs will further enhance the efficacy of immunotherapy of DLBCL. In conclusion,
341 this study shows DuoHexaBody-CD37 induces cytotoxic signaling in DLBCL cells, and reduces
342 cytokine-mediated pro-survival signaling in the DLBCL tumor microenvironment.
343
344
345
346
347
348
349

350 # Material and Methods

351 **Therapeutic antibodies**

352 DuoHexaBody-CD37 (GEN3009) and the negative control anti-HIV-1 gp120 antibody IgG1-b12
353 (mentioned in manuscript as IgG1-ctrl) were generated by Genmab (Utrecht, The
354 Netherlands) as previously described [61]. Rituximab anti-CD20 (Mab Thera®) was obtained
355 from Radboudumc (Nijmegen, the Netherlands).

356

357 **Cell culture**

358 Lymphoma cell lines (GCB-DLBCL: Oci-Ly8, Oci-Ly7; ABC-DLBC: HBL-1, U2932; B-ALL: NALM6,
359 and Burkitt: BJAB, DAUDI) were obtained from DSMZ, ATCC, Blanca Scheijen (Dept.
360 Pathology, Radboudumc) and Marcel Spaargaren (Dept. of Pathology, AmsterdamUMC) and
361 cell lines were authenticated using STR-analysis. Cells were cultured in RPMI 1640 (Gibco),
362 1% antibiotic-antimycotic (Gibco) and 10% FBS (Hyclone) (RPMI/10%FCS) and incubated at
363 37°C with 5% CO_2. For optimum growth, the cell lines were propagated in dilution of 0.5 ×
364 10^6 cells/ml and the culture media were refreshed twice a week. All experiments were
365 performed one day after refreshing medium and expanding cell culture.

366

367 **MTS assay**

368 Cell viability was determined using CellTiter 96® AQueous One Solution Reagent from
369 Promega as per manufacturer instructions. Briefly, $2x10^5$ cells in RPMI/10%FCS were plated
370 in 96-well plates and treated with 5µg/ml DuoHexaBody-CD37 for 30min at 4°C. Cells were
371 washed and treated with 5 µg/ml of goat F(ab')2 anti-human IgG (a-Fc, Southern Biotech)
372 and incubated for 48h at 37°C with 5% CO_2. As control, cells treated with DuoHexaBody-

373 CD37 or a-Fc alone were included. Subsequently, cells were stained with 1:5 dilution of
374 CellTiter 96® AQueous One Solution Cell Proliferation Assay (MTS, Promega) in media
375 (RPMI/10%FCS) and incubated at 37°C with 5% CO_2 for 2-3hrs. Absorbance was recorded at
376 490nm in a 96-well plate reader (Bio-Rad iMark Microplate Absorbance Reader).

377

378 **Cytotoxicity assays**

379 Peripheral blood from healthy volunteers was obtained via Sanquin blood bank (Nijmegen,
380 NL) upon informed consent and anonymized for further use, following the guidelines of the
381 Institutional Review Board, and in accordance with the declaration of Helsinki. Peripheral
382 blood mononuclear cells (PBMCs) were isolated using Ficoll Hypaque (GE Healthcare, Little
383 Chalfont, UK) according to the manufacturer's instructions. For studying different subsets of
384 FcγR-expressing cell types, B cell, T cells, monocytes and NK cells were isolated using Miltenyi
385 Biotec cell separation reagents (130-101-638, 130-096-495, 130-117-337 and 130-092-657,
386 respectively). For fixation, PBMCs and the purified immune cell subsets were washed with
387 PBS and resuspended directly in 1%PFA (filter sterilized) at $7.5x10^6$ cells/ml for 20min at RT
388 (room temperature). Following, cells were washed twice in PBS and resuspended in media
389 (RPMI/10%FCS). In parallel, $10x10^6$ target cells (HBL-1 or U2932) were stained with CellTrace
390 Violet Cell Proliferation Kit (Invitrogen) at final concentration of 167nM for 20min at 37°C
391 with 5% CO_2. Subsequently, cells were washed twice and resuspended in media
392 (RPMI/10%FCS). Next, CTV-stained target cells were treated with 5µg/ml DuoHexaBody-
393 CD37 for 30min at 4°C and washed with media. In addition, target cells were co-cultured
394 with fixed PBMCs at 1:20 (target to crosslinker) ratio for 4, 24 or 48h (or for 3 hours with the
395 purified immune cell subsets), at 37°C in the presence of 5% CO_2. Subsequently, cells were

396 directly stained with 5µg/ml propidium iodide (Miltenyi Biotec) for 5min at RT on plate
397 shaker and analyzed using FACS Lyric (BD Biosciences).
398
399 **Target binding analysis**
400 Briefly, 100,000 lymphoma cells (HBL-1, Oci-Ly7, U2932, BJAB or DAUDI) were treated with
401 5mg/ml of anti-CD20 Rituximab (Mab Thera®) or DuoHexaBody-CD37 in RPMI/0.2%BSA for
402 15min at RT in a 96-wells plate. Plates were then directly transferred to incubator (37°C/5%
403 CO_2) for 0, 2 or 6h. Cells were harvested at respective time points by washing with PBA buffer
404 (PBS, 1% BSA, azide 0.02%) followed by staining with mouse anti-human IgG1 Fc secondary
405 antibody conjugated to Alexa Fluor 488 (ThermoFisher) for 30min at 4°C. Next, cells were
406 washed and stained with Live-dead marker (eFluor 506, eBioscience) and measured using
407 FACS Lyric (BD Biosciences).
408
409 **Generation of CD37 mutant cell lines**
410 NALM6 cells were used because of their endogenous low CD37 expression. Cells were grown
411 in RPMI/10% FBS supplemented with glutamine 2mM. Cells were transfected with either
412 CD37-sGFP2, CD37 Y13F-sGFP2 or CD37-delta Y13-sGFP2 constructs using the Amaxa 4D
413 nucleofector. Briefly, for each transfection $3x10^6$ cells were collected and washed with PBS.
414 Cells were resuspended in 100 µl SF buffer (cat. no. V4XC-2024) containing 3 µg of plasmid
415 and pulsed with program CV-104. After transfection, cells were transferred to 6-well plates
416 and incubated overnight in 3 ml of RPMI with 10% FBS without antibiotic-antimycotic and
417 phenol red. The CD37 constructs were kindly provided by Prof. Dr. N. Muthusamy (Ohio
418 University, USA) [27], and subcloned in pSGFP-N1 vector using standard techniques. Sequences
419 were verified via sequencing.

420 **Phosphoflow assays**

421 Lymphoma cells ($2x10^5$ cells/well) or PBMCs ($5x10^5$ cells/well) in RPMI/10%FCS were treated
422 with 5µg/ml DuoHexaBody-CD37 for 30min at 4°C. Next, cells were washed and treated with
423 5µg/ml of goat F(ab')2 anti-human IgG (a-Fc) and incubated for 20min at 37°C with 5% CO_2.
424 As treatment control, cells were treated with DuoHexaBody-CD37 or a-Fc alone. As positive
425 control of B-cell receptor stimulation, cells were treated with 20µg/ml of goat F(ab')2
426 antihuman IgM. Next, cells were spun down and stained at 1:10 dilution with Fixable Viability
427 stain 510 (BD Biosciences) in RPMI/10%FCS for 10min at 37°C. Thereafter, cells were directly
428 fixed for 10min at 37°C with 100 µl of the eBioscience FoxP3/Transcription Factor Fixation kit
429 (Invitrogen) as indicated by the manufacturer. After fixation, samples were washed twice
430 with eBioscience Permeabilization Wash Buffer (10X diluted in Milli-Q) (Invitrogen). To
431 identify the B cells within PBMC cultures, cells were stained with antibodies against CD19,
432 CD3 and IgD diluted in eBioscience wash buffer. To prevent non-specific antibody binding,
433 FcR-blocking purified rat anti-mouse CD16/CD32 (Mouse BD Fc BlockTM) was included in the
434 staining. Stained cells were incubated for 30min at 4°C followed by washing in eBioscience
435 wash buffer and staining with antibodies against phosphorylated proteins; p-SHP1(Y564), p-
436 AKT(S473), p38(T180/Y182) (all Cell signaling technology), p-SYK(Y348), p-BTK(Y223),
437 pPLCγ2(Y759), p-PKCα/βII(T638/641), p-ERK-1/2(T202/Y204) (all BD Biosciences); in wash
438 buffer for 30min at RT. Unlabeled phospho-antibodies (p-SHP1(Y564), p-AKT(S473),
439 p38(T180/Y182)) were stained with a secondary PE-labeled F(ab')2 donkey anti-rabbit IgG
440 (H+L) antibody (Jackson Immuno Research) for 15min at RT. Lastly, the cells were washed and
441 resuspended in wash buffer before measuring on FACS Lyric.

442

443 **Cytokine stimulation experiments**

444 To measure p-STAT3 and p-STAT6 responses, cells treated with DuoHexaBody-CD37 and/or goat
445 F(ab')2 anti-human IgG (a-Fc) for 24h as described above. After washing, cells were
446 stimulated with recombinant IL-6 (100ng/ml) or IL-4 (20ng/ml) (both from Miltenyi) or IL-21
447 (Peprotech) (50ng/ml) for 15min at 37°C. Cells were harvested and stained with Fixable
448 Viability stain 510 (BD Biosciences). Subsequently, cells were fixed with BD Cytofix Fixation
449 Buffer (BD Biosciences) for 10min at 37°C and washed twice with MACS buffer (PBS/0.5%
450 BSA/2 mM EDTA). Next, cells were permeabilized using 150 µl Perm Buffer III (BD
451 Biosciences) at 4°C for 30min and washed twice with MACS buffer, followed by staining with
452 PE-labeled p-STAT3 (Y705) or p-STAT6 (Y641) (BD Biosciences) antibody diluted (1:8) in MACS
453 buffer for 30min at RT. Finally, the cells were washed and resuspended in 50 µl MACS buffer
454 before measuring on FACS Lyric.

455

456 **Supplementary methods:** Microscopy analysis of CD37 clustering, RPPA assay,
457 DuoHexaBody-CD37 surface accessibility assays, CRISPR-cas9 knockout of SHP1 in DLBCL cell
458 lines and quantification of apoptosis.

459

Acknowledgements

We thank the Radboudumc Microscopy Imaging Center for use of their microscopy facilities, as well as for their support and assistance. We thank Simone Oostindie and Inge Verbrugge for valuable scientific input, and Peter Friedl for facilitating the RPPA studies. The CD37 constructs were kindly provided by Natarajan Muthusamy (Ohio University, USA) [27].

Disclosures

MGR, MBO, KCMS and ECWB are Genmab employees and own Genmab warrants and/or stock. All the other authors have no conflicts of interest to disclose. This research study was funded by Genmab, and we acknowledge funding support from the Netherlands Organization for Scientific Research (NWO) Gravitation programme IMAGINE! (project 24.005.009), the Institute of Chemical Immunology (project ICI00023), ZonMW (project 09120012010023), the Dutch Cancer Society (projects 12949 and 14726), and the European Research Council: Consolidator Grant (project 724281) and Proof-of-Concept Grant (project 101112687).

Author contributions

ABvS, SPS, ECWB, MGR, KCMS and MBO provided scientific input and conceptualized the study. SPS developed the methodology and performed the data analysis for the cytotoxicity assays, PBMC assays, phosphoflow experiments, CD37 mutant studies, cytokine studies and RPPA analysis. KM performed FcγR cytotoxicity studies, CD37 expression studies and apoptosis assays. MDvdB performed the surface accessibility assays and CD37 mutant studies. SvD developed the methodology for the CD37 transfections. MTB developed

483 methodology of CD37 microscopy studies and performed data analysis on CD37 clustering.
484 WC generated and validated the SHP-1 KO cells and performed cytotoxicity assays. SPS and
485 ABvS wrote the manuscript. ABvS supervised the study. All authors read, revised, and agreed
486 on the final version of the manuscript.

487 # Figure legends

488 **Figure 1: DuoHexaBody-CD37-induces direct cytotoxicity in DLBCL-derived tumor cell lines**

489 **(A)** Percentage decrease (mean +/- SD) in viability upon DuoHexaBody-CD37 treatment in
490 presence or absence of goat F(ab')2 anti-human IgG (a-Fc) in indicated cell lines after 48h.
491 Data is shown from at least three independent experiments. Significance was calculated
492 compared to untreated control using Kruskal-Wallis test followed by Dunn' multiple
493 comparison test correction (**p<0.01) **(B)** Percentage increase in cell death (PI-positive)
494 upon co-culturing healthy donor-derived fixed PBMCs with DuoHexaBody-CD37 pre-treated
495 HBL-1 and U2932 cells compared to untreated cells for indicated time points. Duplicates
496 from each individual donor (n=4) are indicated in separate colors. Significance was calculated
497 compared to 4h treated cells using Kruskal-Wallis test followed by Dunn' multiple
498 comparison test correction (*p<0.05, **p<0.01, ***p<0.001). **(C)** Percentage of cell death in
499 DuoHexaBody-CD37 pre-treated Oci-Ly8 cells (eFluor780-positive) upon co-culturing with
500 healthy donor-derived fixed PBMC, monocytes, NK cells, B cells and T cells compared to Fc-
501 crosslinker. Measurements from three individual donors (mean +/- SD) are shown, with each
502 donor represented by a distinct colored symbol.

503

504 **Figure 2: DuoHexaBody-CD37 induces CD37 clustering without modulating CD37 cell**
505 **surface expression**

506 **(A,B)** Airyscan images depicting clustering (fluorescence/area) upon DuoHexaBody-CD37
507 (DHB-CD37) treatment or B12 isotype control in BJAB **(A)** and Oci-Ly8 **(B)** cells with or
508 without Fc-crosslinking (a-Fc). Data shown from five independent experiments. Bar is 10 µm.
509 Significance was calculated comparing DuoHexaBody-CD37-treated cells to isotype control

510 antibody in the presence and absence of Fc-crosslinking (a-Fc) respectively, using Kruskal-
511 Wallis test followed by Dunn's multiple comparisons test (****p<0.0001, *p<0.05). **(C)**
512 Percentage decrease (mean +/- SD) in cell surface binding by DuoHexaBody-CD37 or
513 rituximab (anti-CD20) in indicated cell lines as measured by flow cytometry. Data is shown
514 from at least three independent experiments. Significance was calculated comparing
515 respective time points using unpaired T-test (*p<0.05, **p<0.01, ***p<0.001).

516

517 **Figure 3: DuoHexaBody-CD37 treatment results in activation of different downstream**
518 **signaling pathways**

519 (**A**) Heatmap depicting log-normalized signal intensities of 26 phosphoproteins with two-fold
520 increase in signal upon DuoHexaBody-CD37 treatment in presence or absence of goat F(ab')2
521 anti-human IgG (a-Fc) in primary B cells, U2932 and Oci-Ly7. (**B**) Oncogenic hallmark
522 signatures obtained from the MSigDB enriched using 26 phosphoproteins with two-fold
523 increase in signal upon DuoHexaBody-CD37 treatment in presence or absence of goat F(ab')2
524 anti-human IgG (a-Fc) in primary B cells, U2932 and Oci-Ly7. (**C**) Phosphoflow analysis of
525 pSYK(Y348), p-SHP1(Y564), p-AKT(S473) on primary B cells (*top row*) or DLBCL cells (*bottom*
526 *row*) either untreated or treated with anti-BCR (F(ab')2 anti-IgM), DuoHexaBody-CD37
527 and/or goat F(ab')2 anti-human IgG (a-Fc). Dot plots depict quantification (mean +/- SD) of
528 mean fluorescence intensity (MFI). Each dot represents individual donor (B cells) or
529 experimental replicate (DLBCL). Significance was calculated compared to untreated control
530 using Kruskal-Wallis test followed by Dunn' multiple comparison test correction (**p<0.01,
531 ***p<0.001, ****p<0.0001).

532

533 **Figure 4: DuoHexaBody-CD37 treatment results in differential activation of BCR and**
534 **RAS/MAPK downstream signaling proteins in primary B cells and DLBCL cell lines**
535 (**A, B**) Phosphoflow analysis of **(A)** p-BTK(Y223), p-PLCγ2(Y759), p-PKCα/βII(T638/641) and **(B)**
536 p38(T180/Y182), p-ERK-1/2(T202/Y204) on primary B cells (*top row*) or DLBCL cells (*bottom*
537 *row*) either untreated or treated with anti-BCR (F(ab')2 anti-IgM), DuoHexaBody-CD37
538 and/or goat F(ab')2 anti-human IgG (a-Fc). Dot plots depict quantification (mean +/- SD) of
539 mean fluorescence intensity (MFI). Each dot represents an individual donor (primary B cells)
540 or experimental replicate (DLBCL cell lines). Significance was calculated compared to
541 untreated control using Kruskal-Wallis test followed by Dunn' multiple comparison test
542 correction (*p<0.05, **p<0.01, ****p<0.0001).
543
544 **Figure 5: CD37 N-terminus is involved in DuoHexaBody-CD37-mediated cytotoxic signaling**
545 (**A**) Histogram showing CD37 cell surface expression determined by flow cytometry analysis
546 of NALM6 cell lines expressing wild type CD37 (CD37-WT), or mutations of Tyr13 to
547 phenylalanine (CD37-Y13F), or deletion of Tyr13 (CD37-ΔY13) in the cytosolic regions of the
548 CD37 molecule. (**B**) p-AKT(S473) and (**C**) p-SHP1(Y564) on NALM6 cell lines transfected with
549 CD37-WT, CD37-Y13F or CD37-ΔY13 treated with DuoHexaBody-CD37 (DHB) and goat F(ab')2
550 anti-human IgG (a-Fc) or crosslinker alone (a-Fc). Dot plots depict p-AKT and p-SHP1 levels in
551 treated (DHB+a-Fc or a-Fc) vs untreated cells in CD37-GFP-positive (transfected) cells using
552 phosphoflow analysis, corrected for background signal from GFP-negative cells. Significance
553 was calculated using Student t-test (*p<0.05). Data shown from three independent
554 experiments.
555

556 **Figure 6: DuoHexaBody-CD37 treatment decreases cytokine-mediated pro-survival**
557 **signaling in DLBCL cell lines**
558 (**A**) Percentages of p-STAT6-positive cells (mean and SD) upon recombinant human IL-4 (rh-
559 IL4) stimulation in DLBCL cells pre-treated with DuoHexaBody-CD37 in presence or absence
560 of goat F(ab')2 anti-human IgG (a-Fc). Data is shown from at least three independent
561 experiments. Percentages of p-STAT3-positive cells (mean +/- SD) upon (**B**) recombinant
562 human IL-6 (rh-IL-6) stimulation in HBL-1 cells (the only IL-6 responsive cell line in this study)
563 or (**C**) recombinant human IL-21 (rh-IL-21) stimulation in DLBCL cells pre-treated with
564 DuoHexaBody-CD37 in presence or absence of a-Fc. Data is shown from at least three
565 independent experiments. (**A-C**) Significance was calculated compared to untreated control
566 using Kruskal-Wallis test followed by Dunn' multiple comparison test correction (**p<0.01).
567
568 **Supplementary Figure 1: Fc-crosslinking-mediated apoptotic cell death induced by**
569 **DuoHexaBody-CD37 is not correlated with CD37 membrane expression**
570 **(A)** Flow cytometric comparison of Annexin V stained, Annexin V + 7AAD stained and
571 unstained cells in presence or absence of DuoHexaBody-CD37, with and without Fc-
572 crosslinking on Oci-Ly8, Oci-Ly7 and HBL 1 cell lines. Data (mean +/- SD) show unstained,
573 Annexin V-positive and Annexin V + 7AAD double positive populations from three
574 independent experiments. **(B)** Flow cytometric quantification of CD37 expressed on
575 membranes of DLBCL and Burkitt cell lines using two different CD37 antibodies (clones WR-
576 17 and M-B371). Data (mean +/- SD) represent three independent experiments. MFI=mean
577 fluorescence intensity.
578

579 **Supplementary Figure 2: Fc-crosslinking does not lead to increased CD37 internalization**
580 **from the cell surface of DLBCL cell lines upon DuoHexaBody-CD37 treatment**

581 Percentage decrease in cell surface binding by DuoHexaBody-CD37 with or without Fc-
582 crosslinker in Oci-Ly8, BJAB, Oci-Ly7, U2932 and DAUDI cell lines as measured by flow
583 cytometry. Data (mean +/- SD) is derived from four independent experiments.
584

585 **Supplementary Figure 3: Principal component analysis of (phospho)protein expression**
586 **profiles after DuoHexaBody-CD37 treatment**
587 Principal component analysis (PCA) of 484 proteins (102 phospho targets and 382 total
588 proteins) in primary B cells (CD19+ purified) and two DLBCL cell lines (Oci-Ly7 and U2932)
589 either untreated or treated with DuoHexaBody-CD37 in presence or absence of a-Fc using
590 reverse phase protein array (RPPA). The first two components of the cluster analysis are
591 shown.
592

593 **Supplementary Figure 4: DuoHexaBody-CD37 treatment results in differential activation of**
594 **BCR and RAS/MAPK downstream signaling proteins in B cells and DLBCL**
595 **(A-C)** Phosphoflow analysis of (A) p-SYK(Y348), p-SHP1(Y564), p-AKT(S473); **(B)** p-BTK(Y223),
596 p-PLCy2(Y759), p-PKCα/βII(T638/641) and **(C)** p38(T180/Y182), p-ERK-1/2(T202/Y204) on
597 primary B cells (*top row*) or DLBCL cells (*bottom row*) either anti-IgM treated or treated with
598 DuoHexaBody-CD37 and/or goat F(ab')2 anti-human IgG (a-Fc). Dot plots depict fold change
599 (mean +/- SD) of mean fluorescence intensity (MFI) of indicated treatment to untreated cells.
600 Each dot represents individual donor (B cells) or experimental replicate (DLBCL). Significance

601 of fold change to untreated control was calculated using Wilcoxon Signed Rank test (*p<0.05,
602 **p<0.01, ****p<0.0001).
603
604 **Supplementary Figure 5: Knockout of SHP1 does not influence DuoHexaBody-CD37**
605 **mediated cytotoxicity**
606 **(A)** Western blot showing SHP-1 levels in Oci-Ly7 and HBL1 cells for parental (NT), empty
607 vector (EV) and SHP-1 gRNA1/gRNA4 transduced cells. Tubulin was used as loading control.
608 **(B)** Percentage of dead (Annexin V + 7AAD double positive) populations in parental,
609 transduction control (gRNA EV), and SHP1 knockout (gRNA SHP1-1 and gRNA SHP1-4) in Oci-
610 Ly7 and HBL1 cells measured by flow cytometry. Data (mean +/- SD) shown from three
611 independent experiments.
612
613
614
615
616
617
618
619
620
621
622
623
624

625

626

627 **References**

628 1. Morin RD, Arthur SE, Hodson DJ. Molecular profiling in diffuse large B-cell lymphoma: why
629 so many types of subtypes? *Br J Haematol*. 2022;196(4):814–29.

630 2. Abou Dalle I, Dulery R, Moukalled N, Ricard L, Stocker N, El-Cheikh J, et al. Bi- and
631 Trispecific antibodies in non-Hodgkin lymphoma: current data and perspectives. *Blood*
632 *Cancer J.* 2024;14(1).

633 3. Johnson NA, Boyle M, Bashashati A, Leach S, Brooks-Wilson A, Sehn LH, et al. Diffuse large
634 B-cell lymphoma: Reduced CD20 expression is associated with an inferior survival. *Blood*.
635 2009;113(16):3773–80.

636 4. Xu-Monette ZY, Li L, Byrd JC, Jabbar KJ, Manyam GC, De Winde CM, et al. Assessment of
637 CD37 B-cell antigen and cell of origin significantly improves risk prediction in diffuse large B-
638 cell lymphoma. *Blood.* 2016;128(26):3083–100.

639 5. Guan XW, Wang HQ, Ban WW, Chang Z, Chen HZ, Jia L, et al. Novel HDAC inhibitor
640 Chidamide synergizes with Rituximab to inhibit diffuse large B-cell lymphoma tumour growth
641 by upregulating CD20. *Cell Death Dis.* 2020;11(1).

642 6. Roschewski M, Staudt LM, Wilson WH. Diffuse large B-cell lymphoma—treatment
643 approaches in the molecular era. *Nat Rev Clin Oncol*. 2013;11(1):12–23.

644 7. Varma G, Goldstein J, Advani RH. Novel agents in relapsed/refractory diffuse large B cell
645 lymphoma. *Hematol Oncol.* 2023;41(S1):92–106.

646 8. Schwartz-Albiez R, Dörken B, Hofmann W, Moldenhauer G. The B cell-associated CD37
647 antigen (gp40-52). Structure and subcellular expression of an extensively glycosylated
648 glycoprotein. *J Immunol* 1988;140(3):905–14.

649 9. Van Spriel AB, De Keijzer S, Van Der Schaaf A, Gartlan KH, Sofi M, Light A, et al. The
650 tetraspanin CD37 orchestrates the α4β1 integrin-Akt signaling axis and supports long- lived
651 plasma cell survival. *Sci Signal*. 2012 ;5(250):ra82.
652 10. de Winde CM, Zuidscherwoude M, Vasaturo A, van der Schaaf A, Figdor CG, van Spriel
653 AB. Multispectral imaging reveals the tissue distribution of tetraspanins in human lymphoid
654 organs. *Histochem Cell Biol*. 2015; 144(2):133-46.
655 11. Berditchevski F, Rubinstein E. Tetraspanins. 2013. 1–418
656 p. http://link.springer.com/10.1007/978-94-007-6070-7 .
657 12. Hemler ME. Targeting of tetraspanin proteins — potential benefits and strategies.
658 *Nat Rev Drug Discov*. 2008;7(9):747–58.
659 13. Querol Cano L, Dunlock VME, Schwerdtfeger F, van Spriel AB. Membrane organization by
660 tetraspanins and galectins shapes lymphocyte function. *Nat Rev Immunol*. 2024 ;24(3):193–
661 212.
662 14. Barrena S, Almeida J, Yunta M, Lopez A, Fernandez-Mosteirin N, Giralt M, et al. Aberrant
663 expression of tetraspanin molecules in B-cell chronic lymphoproliferative disorders and its
664 correlation with normal B-cell maturation. *Leukemia.* 2005;19(8):1376–83.
665 15. Bobrowicz M, Kubacz M, Slusarczyk A, Winiarska M. Cd37 in b cell derived tumors— more
666 than just a docking point for monoclonal antibodies. *Int J Mol Sci*. 2020 ;21(24):1.
667 16. Beckwith KA, Byrd JC, Muthusamy N. Tetraspanins as therapeutic targets in hematological
668 malignancy: A concise review. *Front Physiol*. 2015 Mar 23;6.
669 17. De Winde CM, Veenbergen S, Young KH, Xu-Monette ZY, Wang XX, Xia Y, et
670 al. Tetraspanin CD37 protects against the development of B cell lymphoma. *J Clin*
671 *Invest*. 2016;126(2):653–66.

672 18. Oostindie SC, Van Der Horst HJ, Kil LP, Strumane K, Overdijk MB, Van Den Brink EN, et al.
673 DuoHexaBody-CD37 ®, a novel biparatopic CD37 antibody with enhanced Fcmediated
674 hexamerization as a potential therapy for B-cell malignancies. *Blood Cancer J*. 2020;10:30.
675 19. Deckert J, Park PU, Chicklas S, Yi Y, Li M, Lai KC, et al. A novel anti-CD37 antibody-
676 drug conjugate with multiple anti-tumor mechanisms for the treatment of B-
677 cell malignancies. *Blood.* 2013;122(20):3500–10.
678 20. Beckwith KA, Frissora FW, Stefanovski MR, Towns WH, Cheney C, Mo X, et al. The CD37-
679 targeted antibody-drug conjugate IMGN529 is highly active against human CLL and in a novel
680 CD37 transgenic murine leukemia model. *Leukemia.* 2014; 144(2):133.
681 21. Köksal H, Dillard P, Josefsson SE, Maggadottir SM, Pollmann S, Fane A, et al. Preclinical
682 development of CD37CAR T-cell therapy for treatment of B-cell lymphoma. *Blood Adv*.
683 2019;3(8):1230–43.
684 22. Imai K, Takeuchi Y, Terakura S, Okuno S, Adachi Y, Osaki M, et al. Dual CAR-T Cells
685 Targeting CD19 and CD37 Are Effective in Target Antigen Loss B-cell Tumor Models. *Mol*
686 *Cancer Ther*. 2024;23(3):381–93.
687 23. Caulier B, Joaquina S, Gelebart P, Dowling TH, Kaveh F, Thomas M, et al. CD37 is a safe
688 chimeric antigen receptor target to treat acute myeloid leukemia. Cell Reports Med.
689 2024;5(6).
690 24. Witkowska M, Smolewski P, Robak T. Investigational therapies targeting CD37 for
691 the treatment of B-cell lymphoid malignancies. *Expert Opin Investig Drugs*. 2018;27(2):171–
692 7.
693 25. Oostindie SC, Van Der Horst HJ, Kil LP, Strumane K, Overdijk MB, Van Den Brink EN, et al.
694 DuoHexaBody-CD37 ®, a novel biparatopic CD37 antibody with enhanced Fc mediated
695 hexamerization as a potential therapy for B-cell malignancies. *Blood Cancer J.* 2020;10:30.

696 26. van der Horst HJ, Oostindie SC, Cillessen SAGM, Gelderloos AT, Overdijk MB, Nijhof IS, et
697 al. Potent Preclinical Efficacy of DuoHexaBody-CD37 in B-Cell Malignancies. *HemaSphere*.
698 2021;5(1):e504.
699 27. Lapalombella R, Yeh YY, Wang L, Ramanunni A, Rafiq S, Jha S, et al. Tetraspanin CD37
700 directly mediates transduction of survival and apoptotic signals. *Cancer*
701 *Cell.* 2012;21(5):694–708.
702 28. Fujimura T, Yamashita-Kashima Y, Kawasaki N, Yoshiura S, Harada N, Yoshimura Y.
703 Obinutuzumab in combination with chemotherapy enhances direct cell death in cd20positive
704 obinutuzumab-resistant non-hodgkin lymphoma cells. *Mol Cancer Ther.* 2021 ;20(6):1133–
705 41.
706 29. Mone AP, Cheney C, Banks AL, Tridandapani S, Mehter N, Guster S, et al. Alemtuzumab
707 induces caspase-independent cell death in human chronic lymphocytic leukemia cells
708 through a lipid raft-dependent mechanism. *Leukemia.* 2006;20:272–9.
709 30. Zhao X, Lapalombella R, Joshi T, Cheney C, Gowda A, Hayden-Ledbetter MS, et al.
710 Targeting CD37-positive lymphoid malignancies with a novel engineered small modular
711 immunopharmaceutical. *Blood* 2007;110(7):2569–77.
712 31. Ivanov A, Beers SA, Walshe CA, Honeychurch J, Alduaij W, Cox KL, et al. Monoclonal
713 antibodies directed to CD20 and HLA-DR can elicit homotypic adhesion followed by
714 lysosome-mediated cell death in human lymphoma and leukemia cells. *Blood.*
715 2009;114(20):4157–41.
716 32. Beers SA, French RR, Chan HTC, Lim SH, Jarrett TC, Vidal RM, et al. Antigenic modulation
717 limits the efficacy of anti-CD20 antibodies: Implications for antibody selection. *Blood.*
718 2010;115(25):5191–201.

719 33. Lim SH, Vaughan AT, Ashton-Key M, Williams EL, Dixon S V., Chan HTC, et al. Fc gamma
720 receptor IIb on target B cells promotes rituximab internalization and reduces clinical efficacy.
721 *Blood.* 2011;118(9):2530–40.
722 34. Whittaker KC, Huang RP. Antibody Arrays Methods and Protocols. 2021. 45–54
723 p. http://www.springer.com/series/7651.
724 35. Pal Singh S, Dammeijer F, Hendriks RW. Role of Bruton's tyrosine kinase in B cells and
725 malignancies. *Mol Cancer.* 2018;17(1):1–23.
726 36. Benoit A, Bou-Petit E, Chou H, Lu M, Guilbert C, Luo VM, et al. Mutated RASassociating
727 proteins and ERK activation in relapse/refractory diffuse large B cell lymphoma. *Sci Rep*.
728 2022;12(1).
729 37. Uddin S, Hussain AR, Siraj AK, Manogaran PS, Al-Jomah NA, Moorji A, et al. Role of
730 phosphatidylinositol 3'-kinase/AKT pathway in diffuse large B-cell lymphoma survival. *Blood*.
731 2006;108(13):4178–86.
732 38. Höpken UE, Rehm A. Targeting the Tumor Microenvironment of Leukemia
733 and Lymphoma. *Trends in Cancer.* 2019;5(6):351–64.
734 39. Wang Y, Wang C, Cai X, Mou C, Cui X, Zhang Y, et al. IL-21 Stimulates the expression and
735 activation of cell cycle regulators and promotes cell proliferation in EBV-positive diffuse large
736 B cell lymphoma. *Sci Rep*. 2020;10(1):1–13.
737 40. Jones ELL, Demaria MCC, Wright MDD. Tetraspanins in cellular immunity. *Biochem*
738 *Soc Trans.* 2011;39(2):506–11.
739 41. Wood B, Sikdar S, Choi SJ, Virk S, Alhejaily A, Baetz T, et al. Leukemia & Lymphoma
740 Abundant expression of interleukin-21 receptor in follicular lymphoma cells is associated
741 with more aggressive disease Abundant expression of interleukin-21 receptor in follicular

742 lymphoma cells is associated with more aggressive disease. *Leuk Lymphoma*.
743 2013;54(6):1212–20.
744 42. Zöller M. Tetraspanins: Push and pull in suppressing and promoting metastasis. *Nat Rev*
745 *Cancer.* 2009;9(1):40–55.
746 43. Kumari S, Devi G V, Badana anil, ramesh Dasari V, rao malla rama. CD151-A Striking
747 Marker for Cancer Therapy. *Biomark Cancer*. 2015;(7):7–7.
748 44. Vences-Catalán F, Kuo CC, Rajapaksa R, Duault C, Andor N, Czerwinski DK, et al. CD81 is a
749 novel immunotherapeutic target for B cell lymphoma. *J Exp Med*. 2019 ;jem.20190186.
750 45. Yoshimura T, Miyoshi H, Shimono J, Nakashima K, Takeuchi M, Yanagida E, et al. CD37
751 expression in follicular lymphoma. *Ann Hematol.* 2022;101(5):1067–75.
752 46. Roumenina LT, Daugan M V., Noe R, Petitprez F, Vano YA, Sanchez-Salas R, et al. Tumor
753 cells hijack macrophage-produced complement C1q to promote tumor growth. *Cancer*
754 *Immunol Res*. 2019;7(7):1091–105.
755 47. Nemenoff RA, Markiewski MM. The role of complement in the tumor microenvironment
756 *Fac Rev.* 2021;10(80).
757 48. Luo S, Wang M, Wang H, Hu D, Zipfel PF, Hu Y. How Does Complement Affect
758 Hematological Malignancies: From Basic Mechanisms to Clinical Application. *Front Immunol.*
759 2020;11.
760 49. Song G, Cho WC, Gu L, He B, Pan Y, Wang S. Increased CD59 protein expression is
761 associated with the outcome of patients with diffuse large B-cell lymphoma treated with R-
762 CHOP. *Med Oncol*. 2014;31(7).
763 50. Fowler NH, Cheah CY, Gascoyne RD, Gribben J, Neelapu SS, Ghia P, et al. Role of the
764 tumor microenvironment in mature B-cell lymphoid malignancies.
765 *Haematologica.* 2016;101(5):531–40.

766 51. Singhal S, Rao AS, Stadanlick J, Bruns K, Sullivan NT, Bermudez A, et al. Human Tumor–
767 Associated Macrophages and Neutrophils Regulate Antitumor Antibody Efficacy through
768 Lethal and Sublethal Trogocytosis. *Cancer Res*. 2024 ;84(7):1029–47.
769 52. Bouwstra R, He Y, De Boer J, Kooistra H, Cendrowicz E, Fehrmann RSN, et al.
770 CD47 expression defines efficacy of rituximab with CHOP in non–germinal center B-cell (Non-
771 GCB) diffuse large B-cell lymphoma patients (DLBCL), but not in GCB DLBCL. *Cancer Immunol*
772 *Res*. 2019 ;7(10):1663–71.
773 53. Zhao X, Lapalombella R, Joshi T, Cheney C, Gowda A, Hayden-Ledbetter MS, et al.
774 Targeting CD37-positive lymphoid malignancies with a novel engineered small modular
775 immunopharmaceutical. *Blood.* 2007;110(7):2569–77.
776 54. Rafiq S, Siadak A, Butchar JP, Cheney C, Lozanski G, Jacob NK, et al. Glycovariant antiCD37
777 monospecific protein therapeutic exhibits enhanced effector cell-mediated cytotoxicity
778 against chronic and acute B cell malignancies. *MAbs*. 2013;5(5):723–35.
779 55. Wang J, Xu-Monette ZY, Jabbar KJ, Shen Q, Manyam GC, Tzankov A, et al. AKT
780 Hyperactivation and the Potential of AKT-Targeted Therapy in Diffuse Large B-Cell
781 Lymphoma. *Am J Pathol* 2017;187:1700–16.
782 56. Arribas A, Napoli S, Munz N, Stussi G, Bertoni F. PI3Kδ activation, IL6 over-expression, and
783 CD37 loss cause resistance to naratuximab emtansine in lymphomas. *Blood Adv.* 2024;
784 bloodadvances.2023012291.
785 57. Krause G, Baki I, Kerwien S, Knödgen E, Neumann L, Göckeritz E, et al. Cytotoxicity of the
786 CD37 antibody BI 836826 against chronic lymphocytic leukaemia cells in combination with
787 chemotherapeutic agents or PI3K inhibitors. *Br J Haematol*. 2016;173(5):791–4.

58. Rødland GE, Melhus K, Generalov R, Gilani S, Bertoni F, Dahle J, et al. The Dual Cell Cycle Kinase Inhibitor JNJ-7706621 Reverses Resistance to CD37-Targeted Radioimmunotherapy in Activated B Cell Like Diffuse Large B Cell Lymphoma Cell Lines. *Front Oncol*. 2019;9:1301.

59. Wilson WH, Young RM, Schmitz R, Yang Y, Pittaluga S, Wright G, et al. Targeting B cell receptor signaling with ibrutinib in diffuse large B cell lymphoma. *Nat Med*. 2015;21(8).

60. Wilson WH, Wright GW, Huang DW, Hodkinson B, Balasubramanian S, Fan Y, et al. Effect of ibrutinib with R-CHOP chemotherapy in genetic subtypes of DLBCL. *Cancer Cell.* 2021;39(12):1643-1653.e3.

61. Oostindie SC, Taylor RP, Van Der Horst HJ, Lindorfer MA, Cook EM, Tupitza JC, et al. CD20 and CD37 antibodies synergize to activate complement by Fc-mediated clustering. *Haematologica*. 2019 ;104(9):1841.

Figure 1

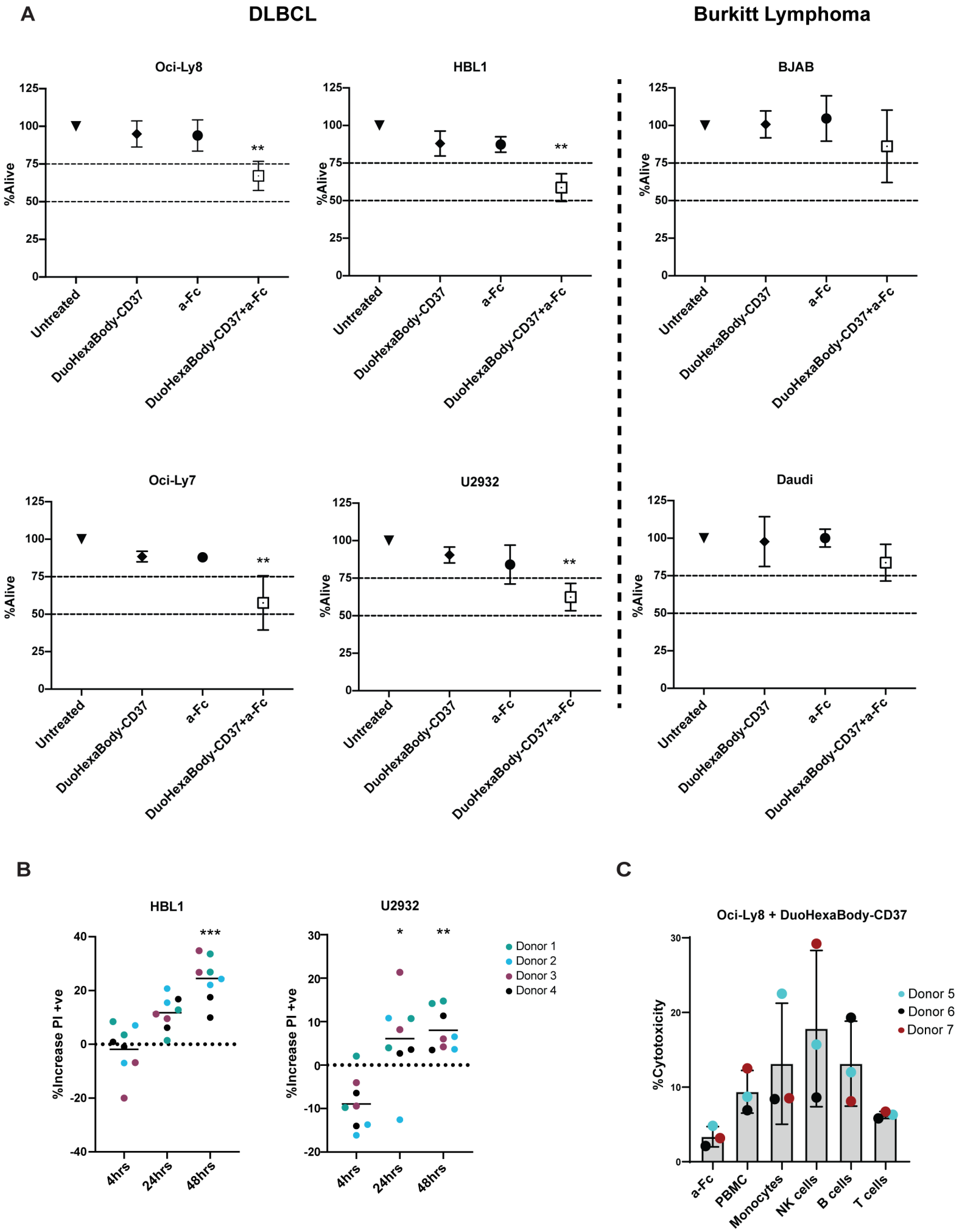
A
DLBCL
Burkitt Lymphoma
Oci-Ly8
HBL1
BJAB
Oci-Ly7
U2932
Daudi
%Alive
125
100
75
50
25
0
**
Untreated
DuoHexaBody-CD37
a-Fc
DuoHexaBody-CD37+a-Fc
B
HBL1
U2932
%Increase PI +ve
40
20
0
-20
-40
***
*
**
4hrs
24hrs
48hrs
Donor 1
Donor 2
Donor 3
Donor 4
C
Oci-Ly8 + DuoHexaBody-CD37
%Cytotoxicity
30
20
10
0
Donor 5
Donor 6
Donor 7
a-Fc
PBMC
Monocytes
NK cells
B cells
T cells

Figure 2

A

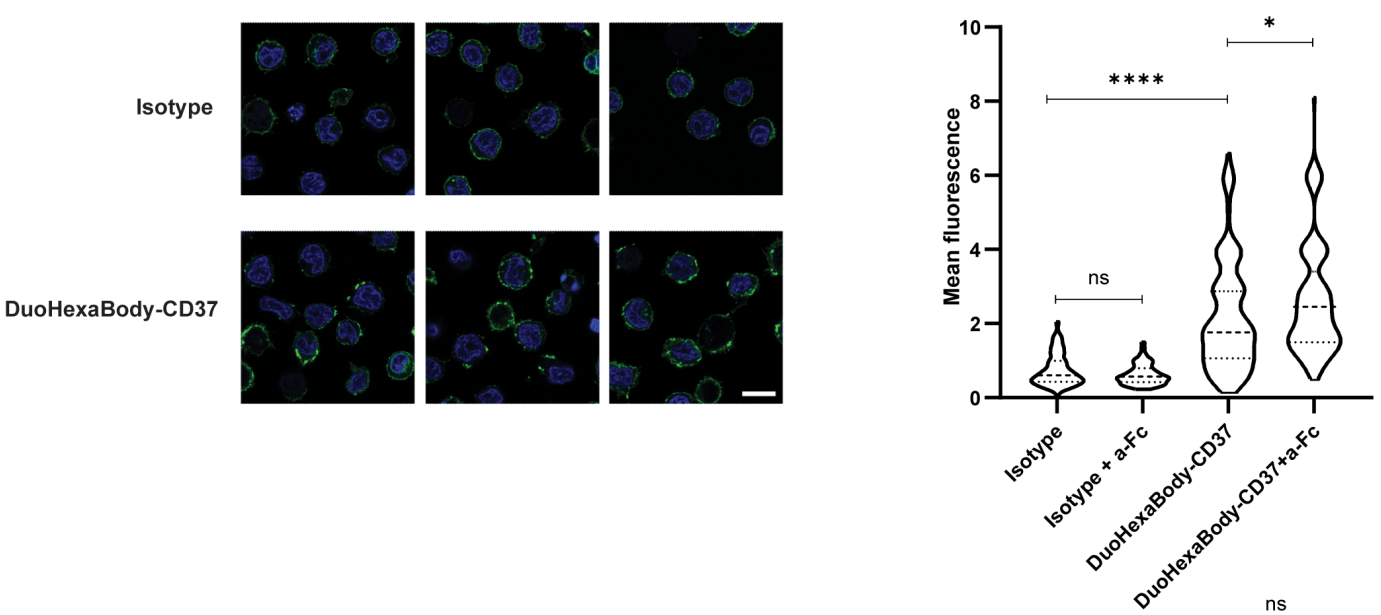
Isotype
DuoHexaBody-CD37
Mean fluorescence
****
*
ns
Isotype
Isotype + a-Fc
DuoHexaBody-CD37
DuoHexaBody-CD37+a-Fc

B

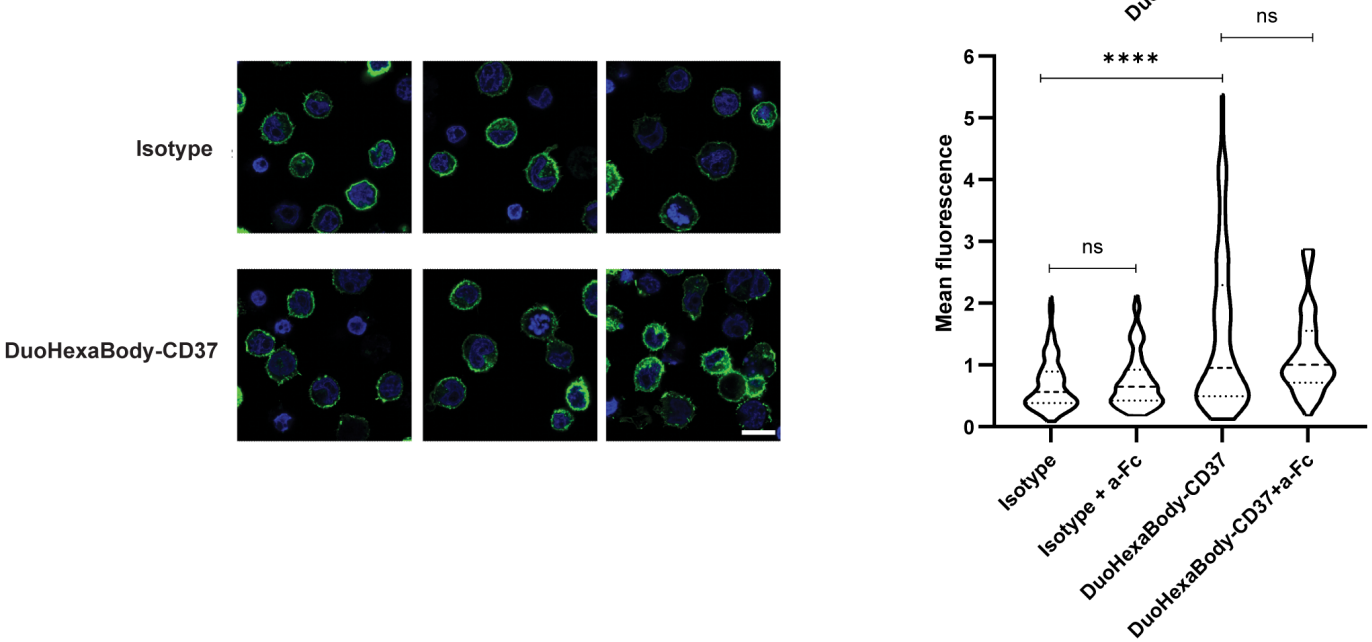
Isotype
DuoHexaBody-CD37
Mean fluorescence
****
ns
ns
Isotype
Isotype + a-Fc
DuoHexaBody-CD37
DuoHexaBody-CD37+a-Fc

C

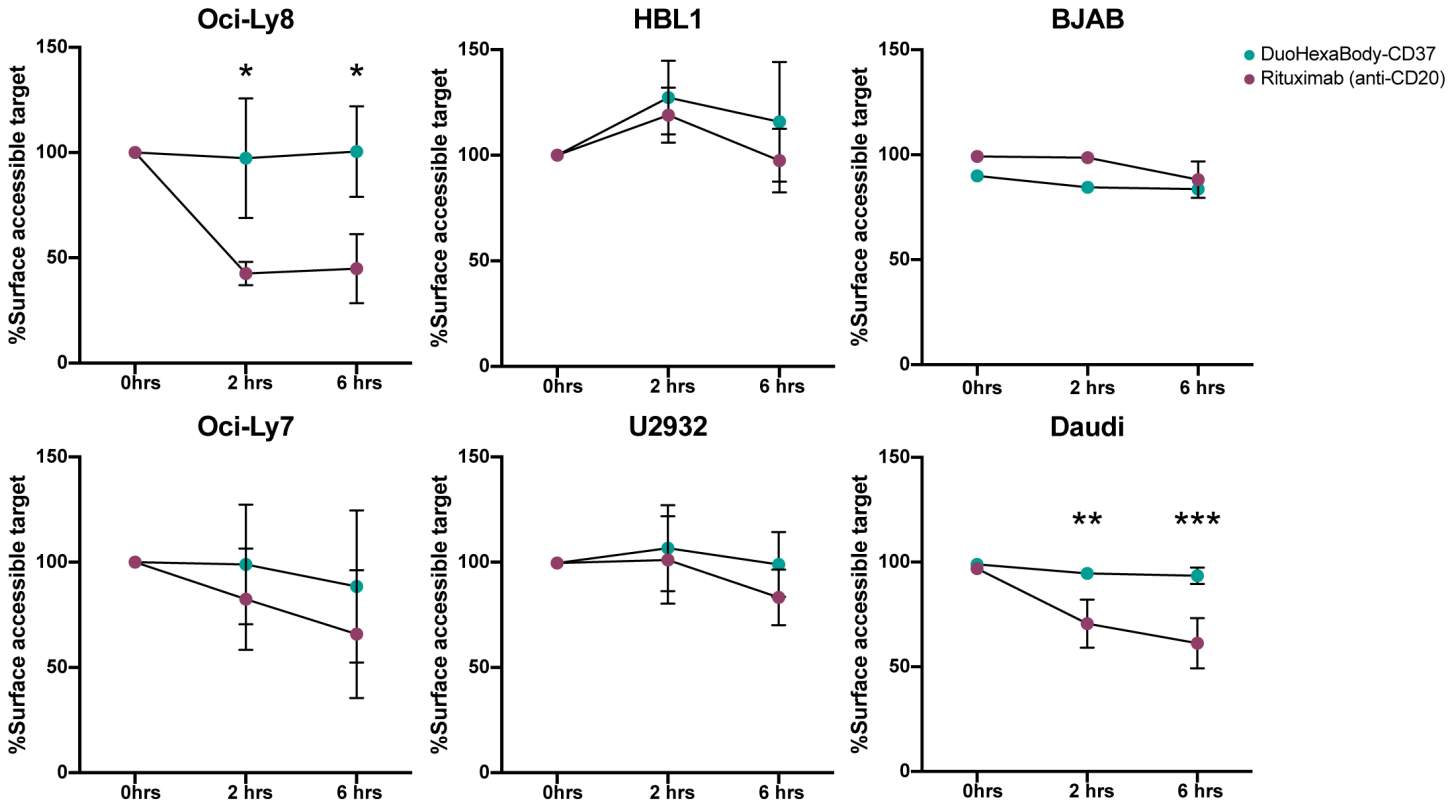
Oci-Ly8
HBL1
BJAB
Oci-Ly7
U2932
Daudi
DuoHexaBody-CD37
Rituximab (anti-CD20)
%Surface accessible target
0hrs
2 hrs
6 hrs
*
**
***

Figure 3

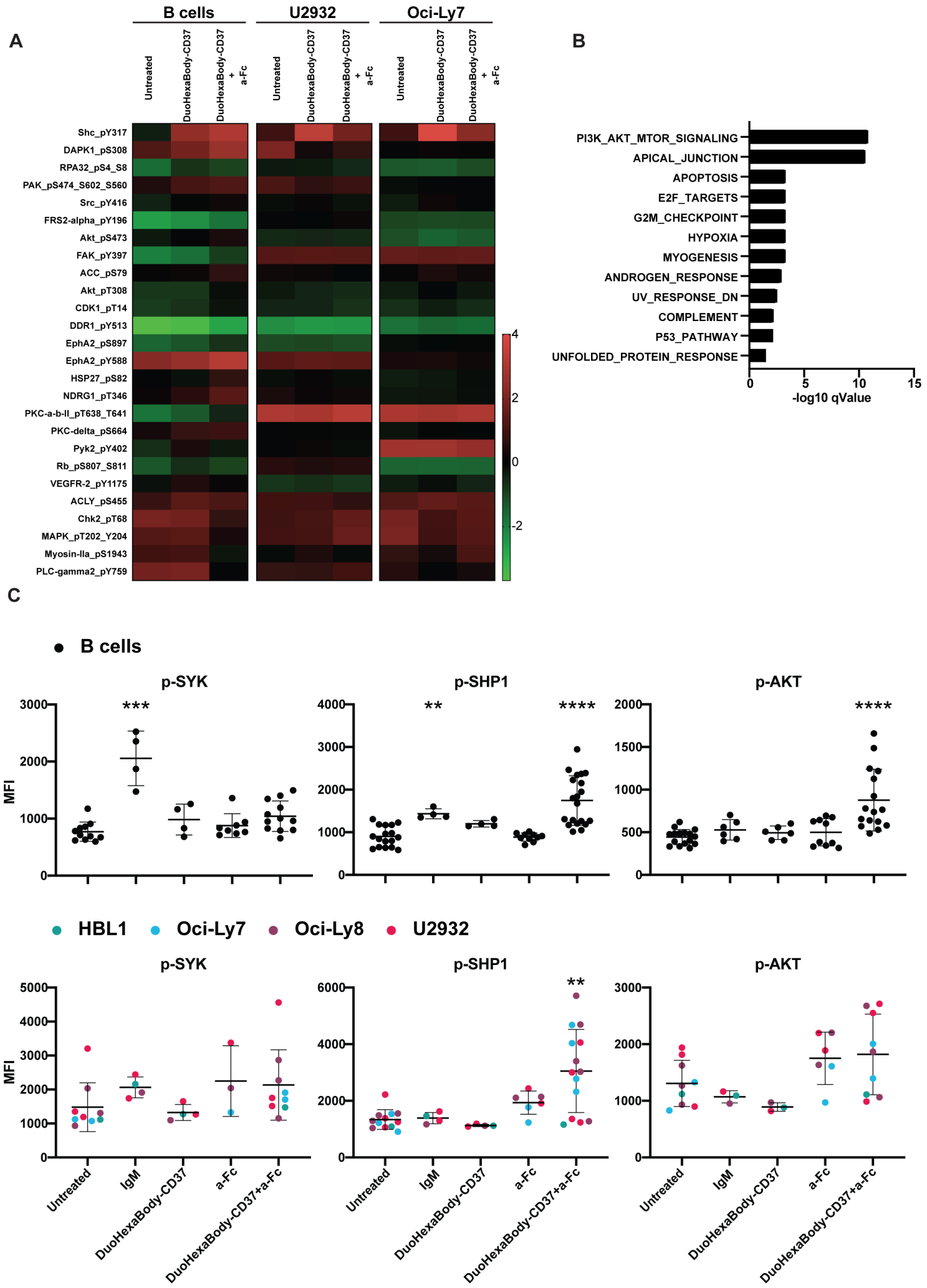
A
B cells
U2932
Oci-Ly7
Untreated
DuoHexaBody-CD37
DuoHexaBody-CD37 + a-Fc
Shc_pY317
DAPK1_pS308
RPA32_pS4_S8
PAK_pS474_S602_S560
Src_pY416
FRS2-alpha_pY196
Akt_pS473
FAK_pY397
ACC_pS79
Akt_pT308
CDK1_pT14
DDR1_pY513
EphA2_pS897
EphA2_pY588
HSP27_pS82
NDRG1_pT346
PKC-a-b-II_pT638_T641
PKC-delta_pS664
Pyk2_pY402
Rb_pS807_S811
VEGFR-2_pY1175
ACLY_pS455
Chk2_pT68
MAPK_pT202_Y204
Myosin-IIa_pS1943
PLC-gamma2_pY759
4
2
0
-2
B
PI3K_AKT_MTOR_SIGNALING
APICAL_JUNCTION
APOPTOSIS
E2F_TARGETS
G2M_CHECKPOINT
HYPOXIA
MYOGENESIS
ANDROGEN_RESPONSE
UV_RESPONSE_DN
COMPLEMENT
P53_PATHWAY
UNFOLDED_PROTEIN_RESPONSE
0
5
10
15
-log10 qValue
C
B cells
p-SYK
p-SHP1
p-AKT
MFI
***
**
****
****
HBL1
Oci-Ly7
Oci-Ly8
U2932
p-SYK
p-SHP1
p-AKT
MFI
**
Untreated
IgM
DuoHexaBody-CD37
a-Fc
DuoHexaBody-CD37+a-Fc

Figure 4

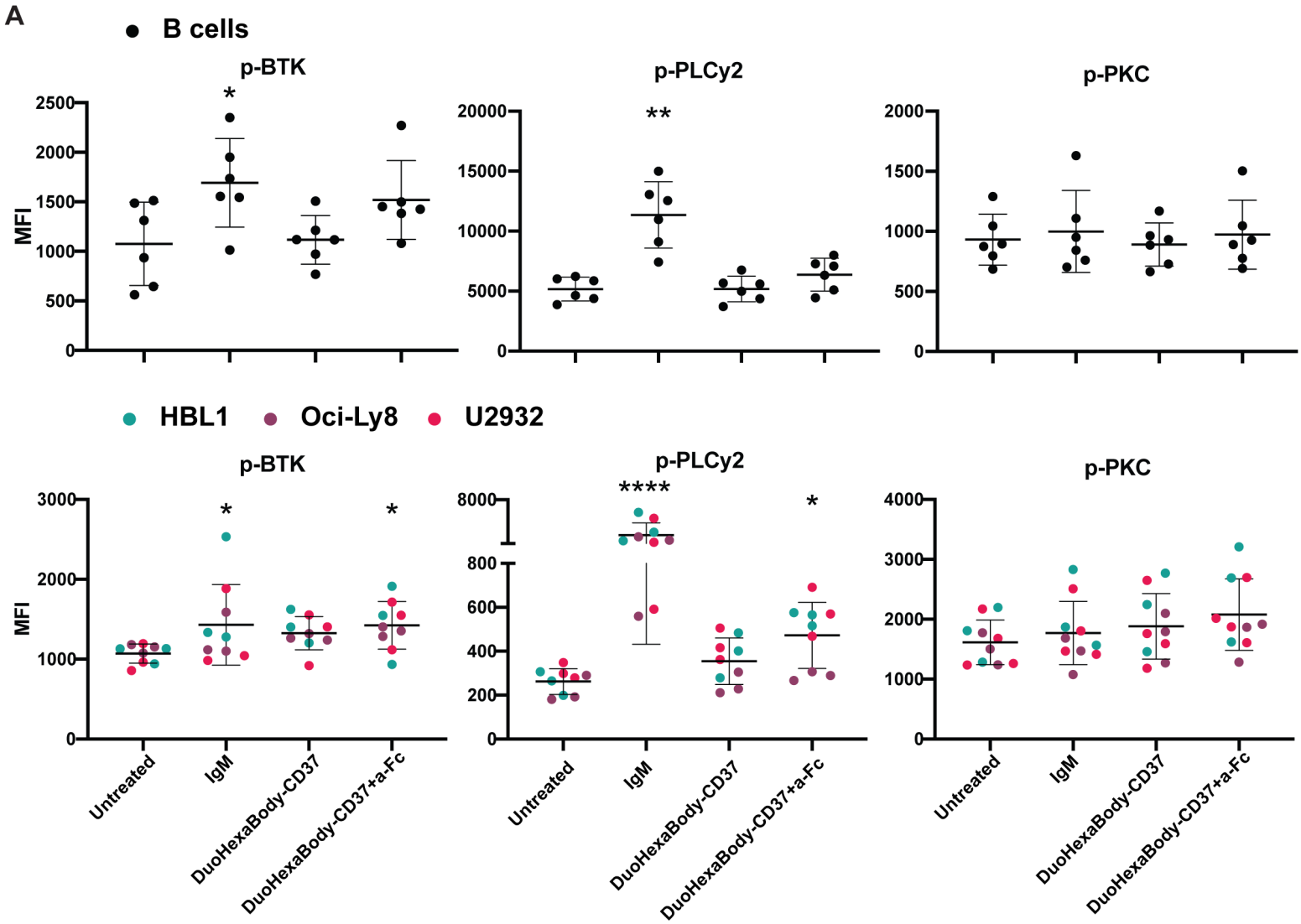
A
B cells
p-BTK
p-PLCy2
p-PKC
MFI
HBL1
Oci-Ly8
U2932
Untreated
IgM
DuoHexaBody-CD37
DuoHexaBody-CD37+a-Fc

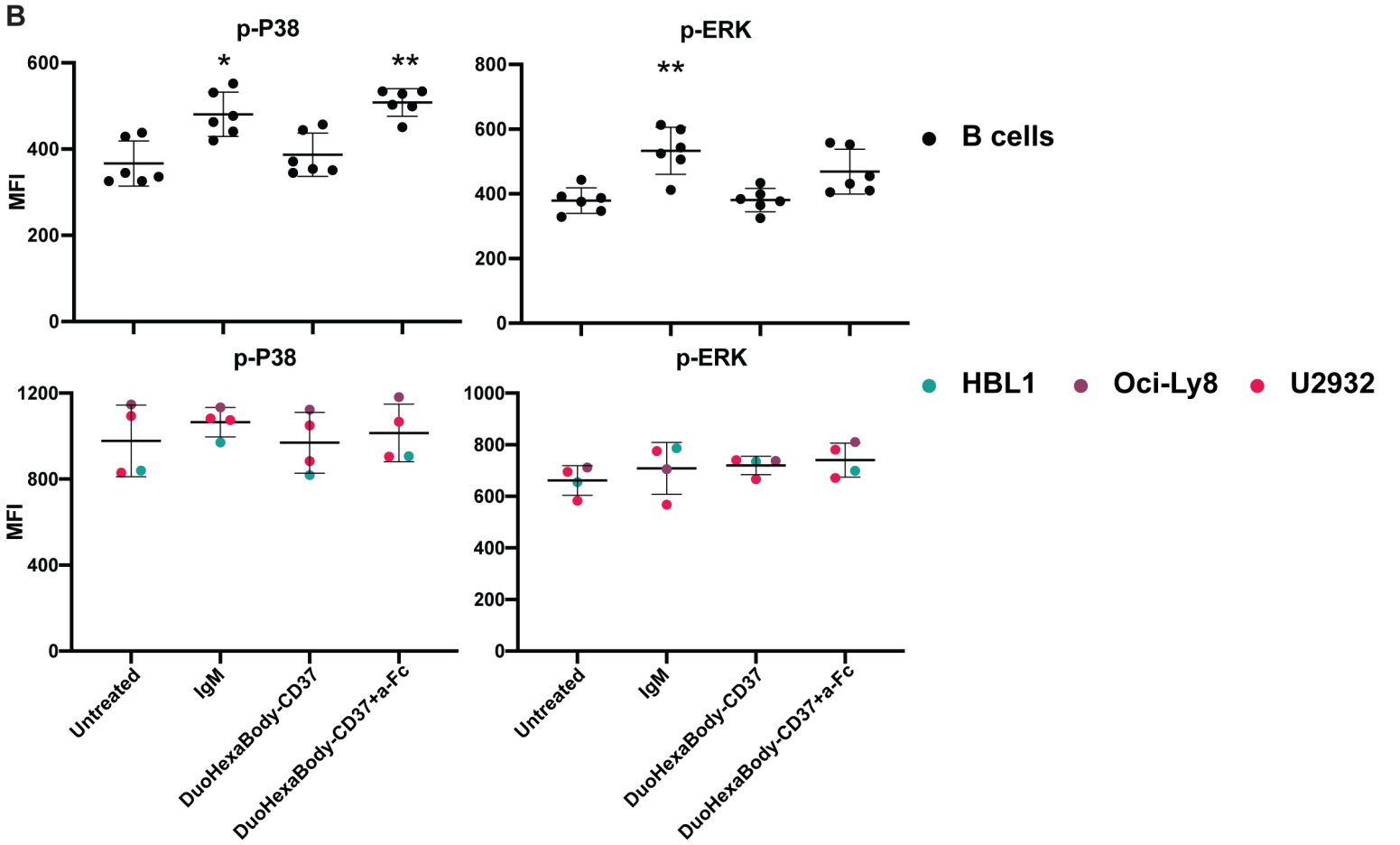
B
p-P38
p-ERK
MFI
B cells
HBL1
Oci-Ly8
U2932
Untreated
IgM
DuoHexaBody-CD37
DuoHexaBody-CD37+a-Fc

Figure 5

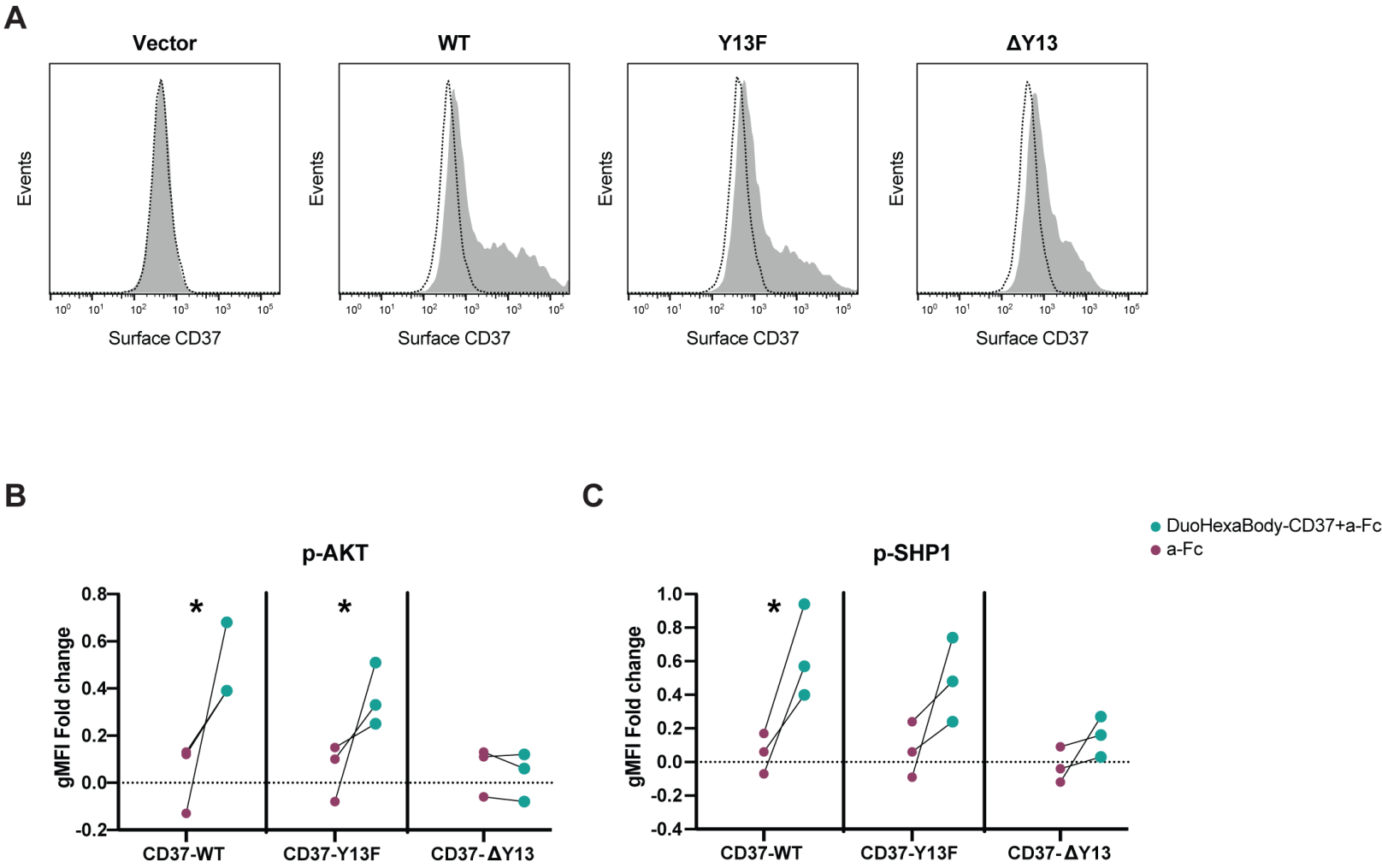
A
Vector
WT
Y13F
ΔY13
Events
Surface CD37
B
p-AKT
gMFI Fold change
0.8
0.6
0.4
0.2
0.0
-0.2
*
*
CD37-WT
CD37-Y13F
CD37-ΔY13
C
p-SHP1
gMFI Fold change
1.0
0.8
0.6
0.4
0.2
0.0
-0.2
-0.4
*
CD37-WT
CD37-Y13F
CD37-ΔY13
DuoHexaBody-CD37+a-Fc
a-Fc

Figure 6

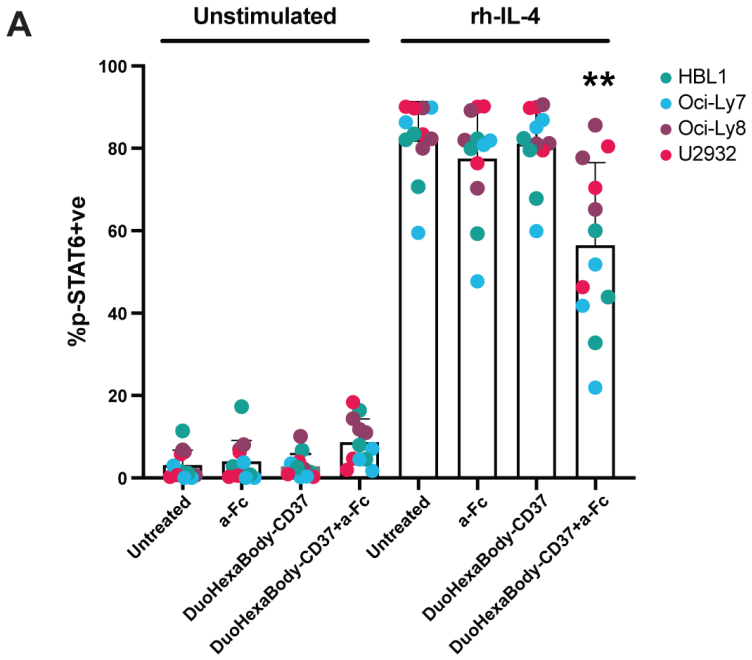
A
Unstimulated
rh-IL-4
%p-STAT6+ve
100
80
60
40
20
0
**
HBL1
Oci-Ly7
Oci-Ly8
U2932
Untreated
a-Fc
DuoHexaBody-CD37
DuoHexaBody-CD37+a-Fc
Untreated
a-Fc
DuoHexaBody-CD37
DuoHexaBody-CD37+a-Fc

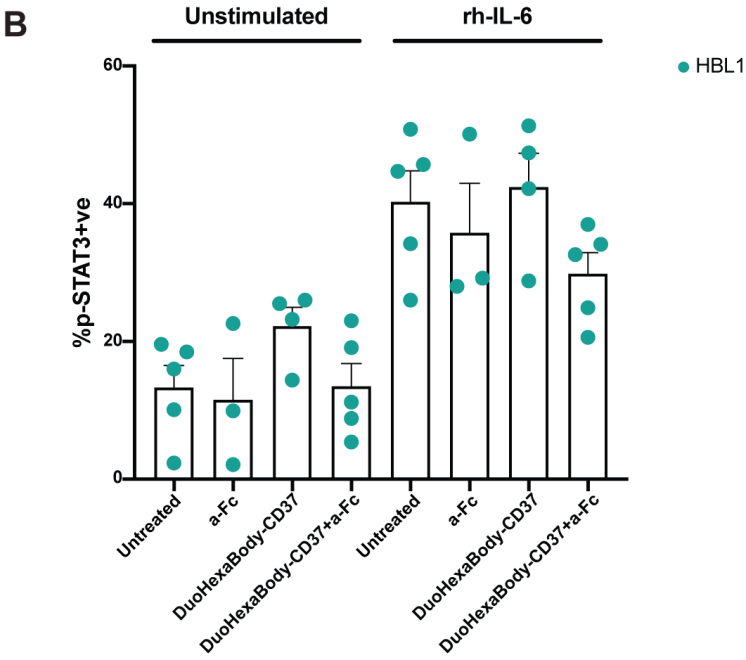
B
Unstimulated
rh-IL-6
%p-STAT3+ve
60
40
20
0
HBL1
Untreated
a-Fc
DuoHexaBody-CD37
DuoHexaBody-CD37+a-Fc
Untreated
a-Fc
DuoHexaBody-CD37
DuoHexaBody-CD37+a-Fc

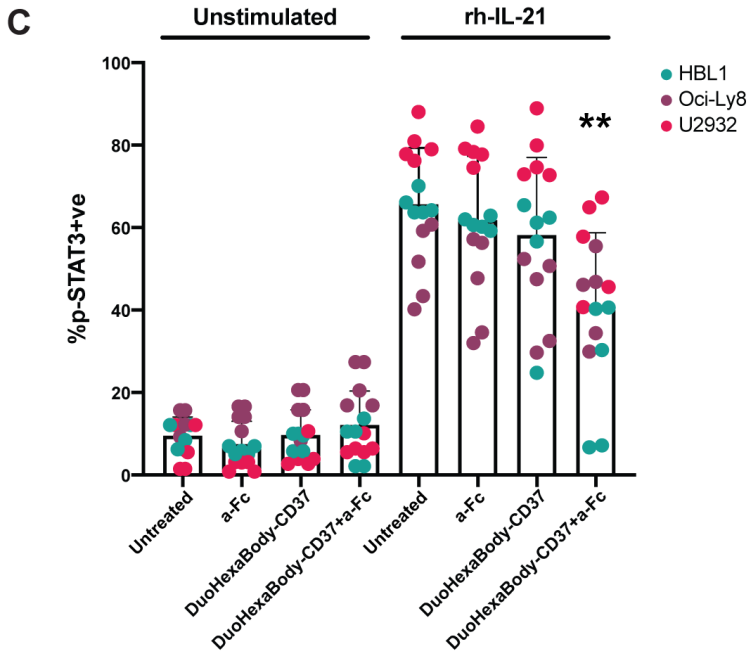
C
Unstimulated
rh-IL-21
%p-STAT3+ve
100
80
60
40
20
0
**
HBL1
Oci-Ly8
U2932
Untreated
a-Fc
DuoHexaBody-CD37
DuoHexaBody-CD37+a-Fc
Untreated
a-Fc
DuoHexaBody-CD37
DuoHexaBody-CD37+a-Fc

Supplementary figure 1

A

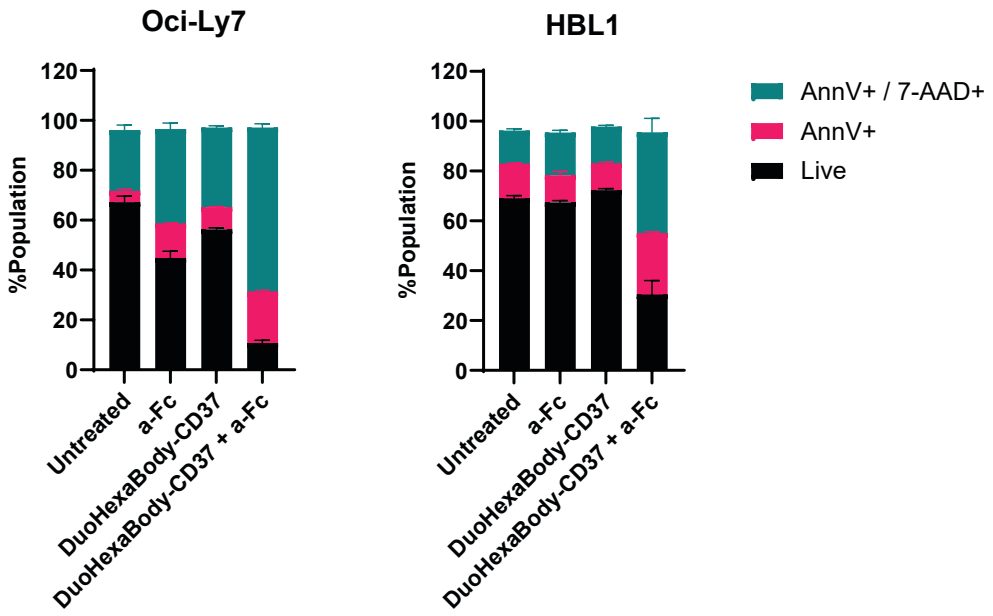

B

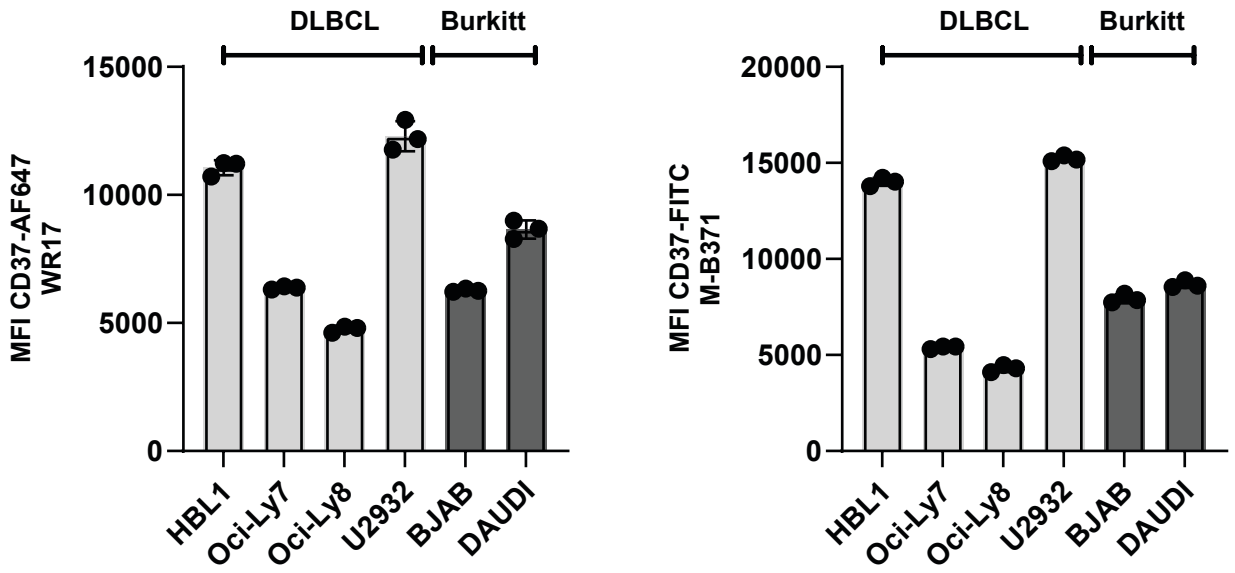

Supplementary figure 2

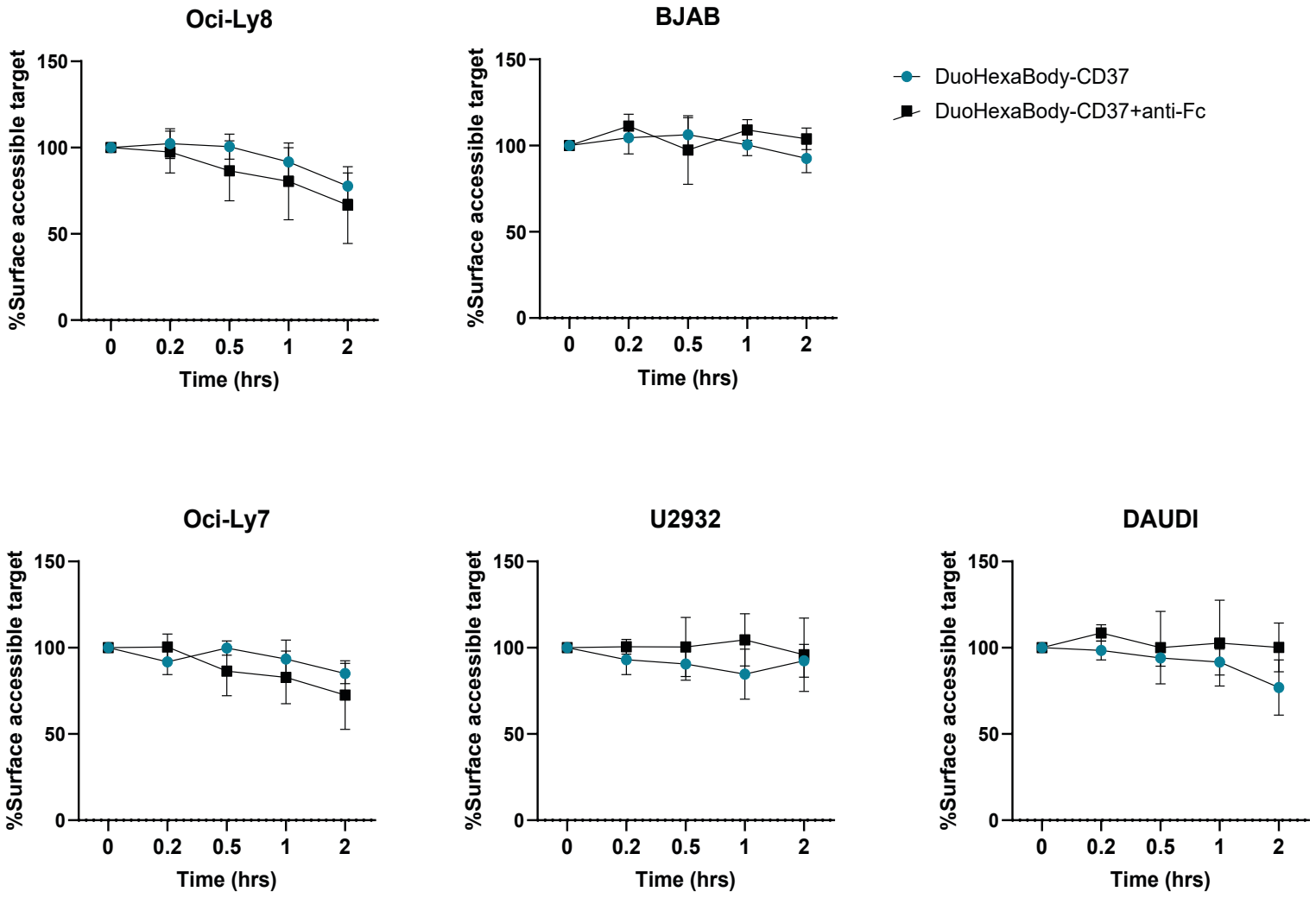

Supplementary figure 3

A

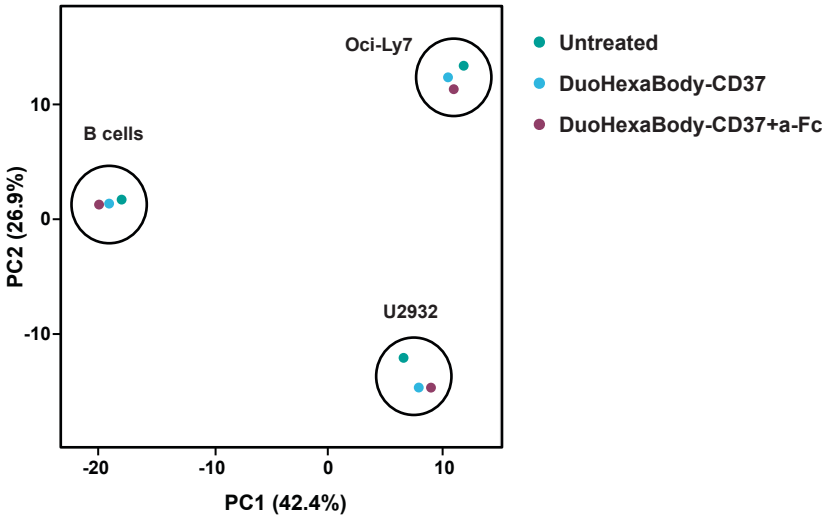

Supplementary Fig. 4

A

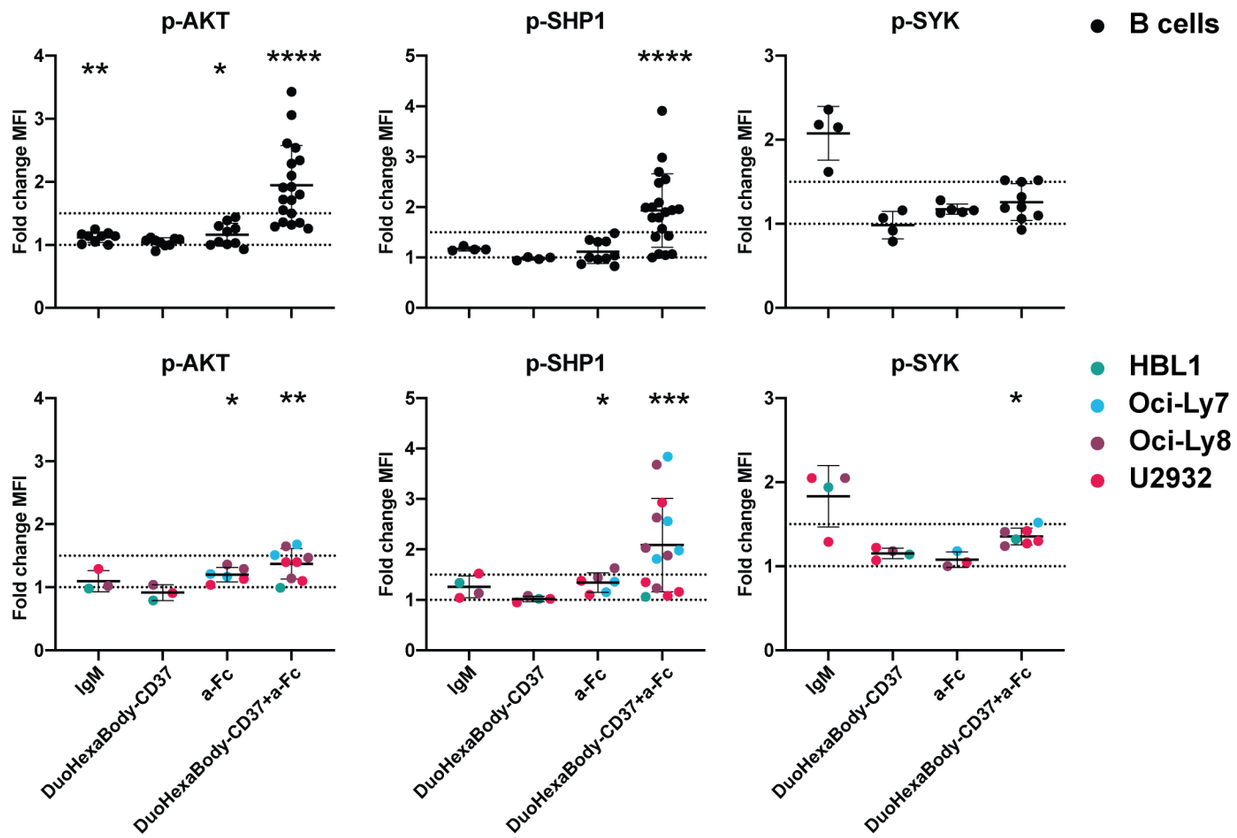

B

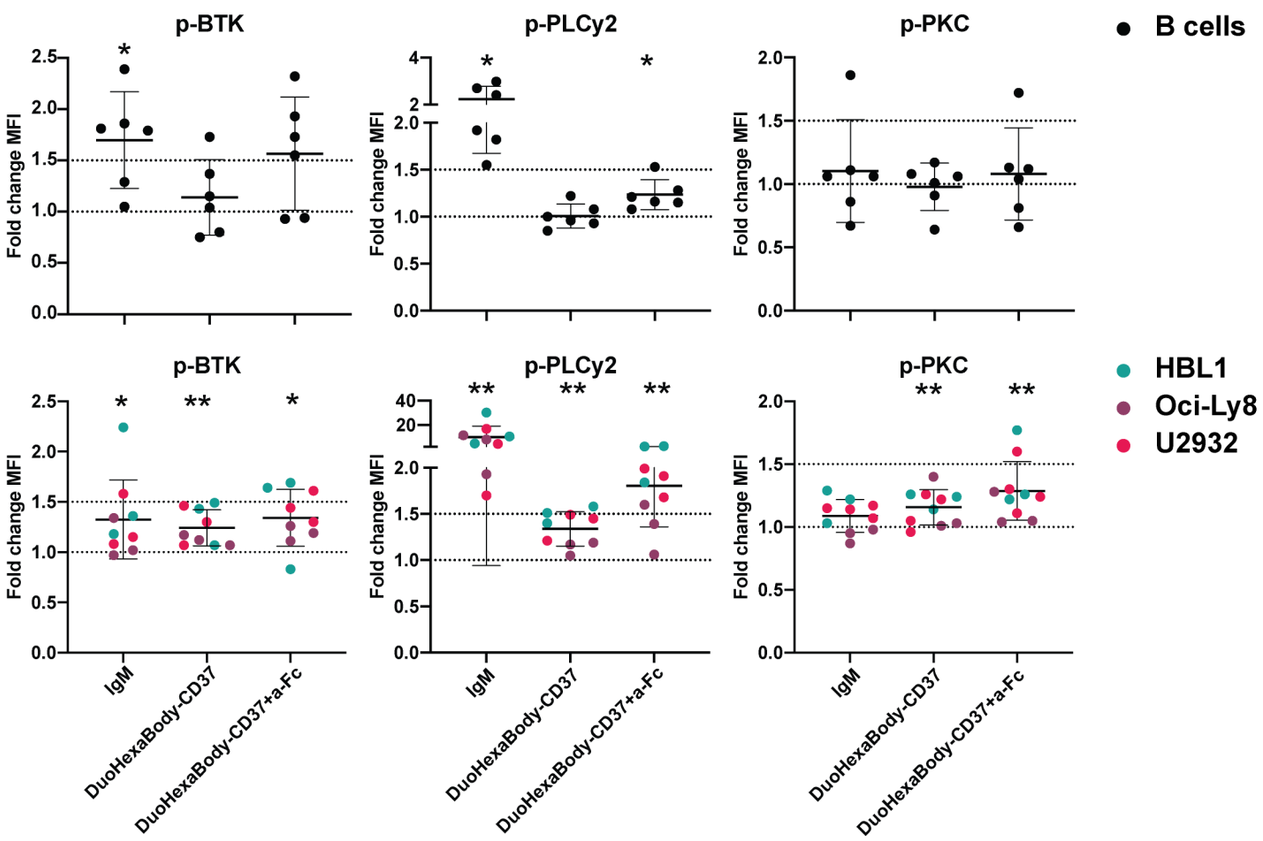

C

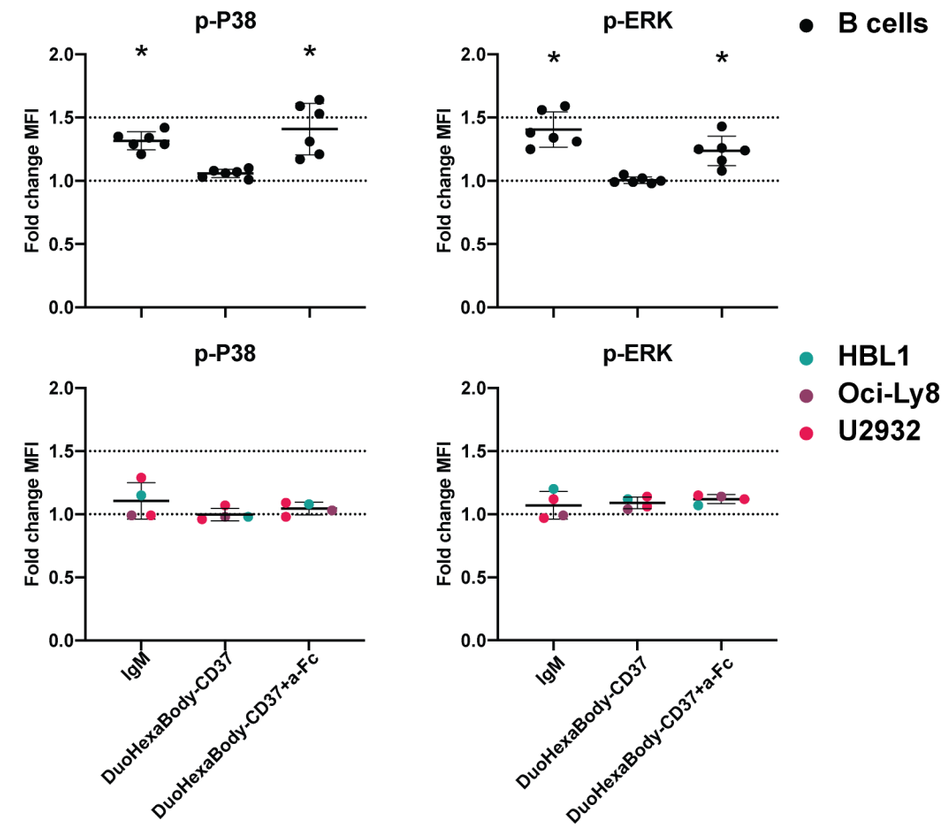

Supplementary figure 5

A

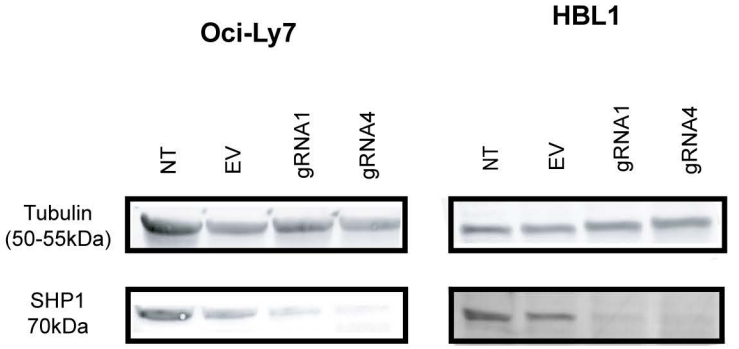

B

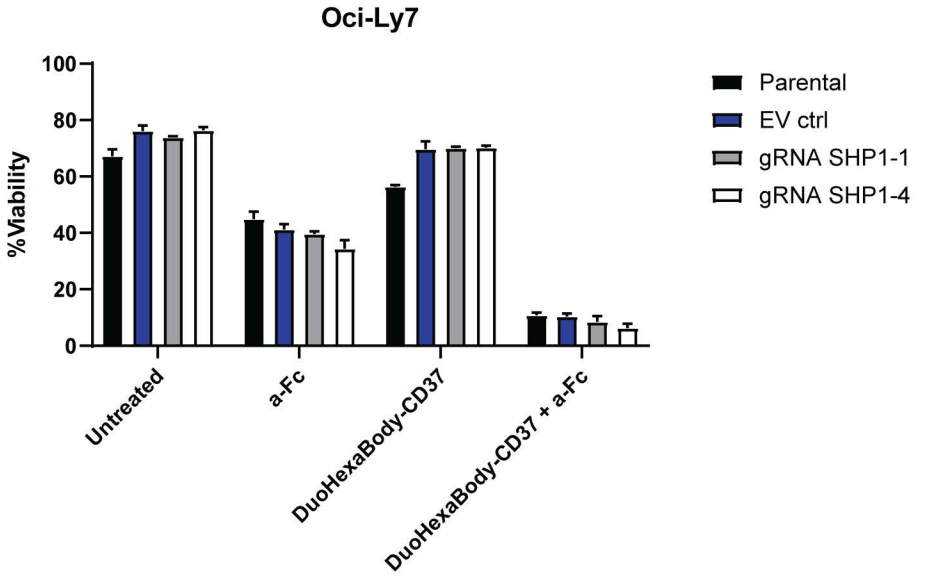

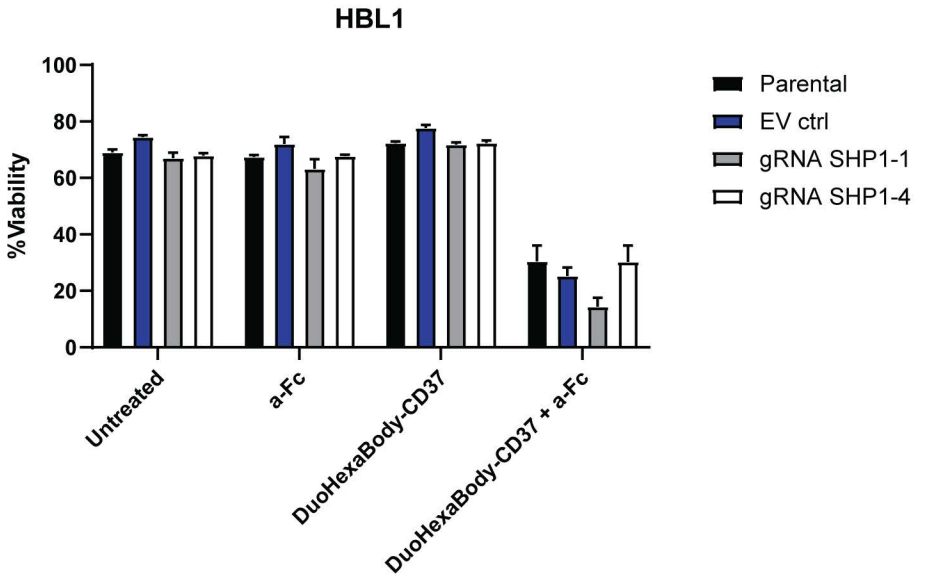

Phosphosite ID	B cells			U2932			Oci-Ly7		
	Untreated	DuoHexaBody-CD37	DuoHexaBody-CD37 +a-Fc	Untreated	DuoHexaBody-CD37	DuoHexaBody-CD37 +a-Fc	Untreated	DuoHexaBody-CD37	DuoHexaBody-CD37 +a-Fc
Shc_pY317	-0,39	2,4	3,02	0,91	3,32	1,83	0,93	4,02	2,28
DAPK1_pS308	1,25	1,37	0,32	0,97	1,03	1,64	1,96	0,91	1,27
RPA32_pS4_S8	1,89	1,78	0,72	0,93	1,05	1,5	1,87	0,96	1,33
PAK_pS474_S602_S560	0,94	1,01	-0,25	-0,14	0,41	-0,13	0,7	0,28	1,1
Src_pY416	1,18	1,85	2,57	2,01	0,24	0,72	0,02	0,17	0,09
FRS2-alpha_pY196	-0,42	-0,09	0,22	-0,15	0,15	-0,2	-0,35	0,2	-0,03
PI3K-p110-a	0,43	-0,87	0,6	0,4	0,44	0,39	-0,37	0,33	0,5
Akt_pS473	-1,64	-0,69	-0,97	-0,29	-0,33	-0,55	-1,27	-1,34	-1,09
FAK_pY397	0,42	1,05	1,17	1,12	0,65	0,86	-0,15	0,05	0,06
ACC_pS79	-2,61	-2,28	-1,76	0,08	-0,04	0,19	-0,98	-1,06	-1,04
Akt_pT308	-0,31	-0,04	0,34	-0,54	-0,47	-0,53	-1,12	-1,47	-1,31
CDK1_pT14	-2	-1,68	-0,86	1,27	1,3	1,29	1,54	1,47	1,53
DDR1_pY513	0,09	0,19	0,66	0,22	0,19	-0,06	0,1	0,37	0,22
EphA2_pS897	-0,75	-0,74	-0,18	-0,31	-0,45	-0,57	-0,37	-0,05	-0,29
EphA2_pY588	-0,84	-0,67	-0,22	-0,47	-0,46	-0,67	-0,66	-0,37	-0,58
HSP27_pS82	-3,68	-3,45	-2,69	-2,23	-2,48	-2,4	-1,71	-1,5	-1,62
NDRG1_pT346	-1,49	-1,22	-0,67	-1,06	-1	-1,1	-0,14	-0,07	-0,11
PKC-a-b-II_pT638_T641	2,2	2,49	3,15	1,33	1,47	1,42	0,31	0,33	0,22
PKC-delta_pS664	-0,03	-0,18	0,68	-0,17	0,13	-0,15	-0,36	-0,27	-0,15
Pyk2_pY402	0,17	0,57	1,31	0,34	0,17	0,22	-0,28	-0,24	-0,17
Rb_pS807_S811	-1,75	-1,31	-0,47	2,99	2,88	3,26	2,95	2,83	2,99
VEGFR-2_pY1175	0,27	0,79	0,89	0,02	-0,11	-0,11	-0,23	-0,1	-0,06
ACLY_pS455	1,82	1,88	0,05	0,74	0,69	1	0,54	0,08	0,29
Chk2_pT68	-0,62	0,37	-0,31	0,01	0,18	-0,16	2,73	2,74	2,48
MAPK_pT202_Y204	-1,24	-0,63	-0,95	0,56	0,42	0,52	-1,48	-1,5	-1,49
Myosin-IIa_pS1943	-0,2	0,47	0,15	-0,73	-0,63	-0,75	-0,34	-0,16	-0,45
PLC-gamma2_pY759	0,82	1,38	1,13	0,96	0,92	0,65	1,22	1,52	1,31

Supplementary Table 1